VOLUME 38 1960

The Canadian Journal of Chemical Engineering

formerly

CANADIAN JOURNAL OF TECHNOLOGY

Published by

THE CHEMICAL INSTITUTE OF CANADA

48 RIDEAU ST. OTTAWA 2

Volume 38 February, 1960 Number 1

The Canadian Journal of Chemical Engineering

formerly

CANADIAN JOURNAL OF TECHNOLOGY

CONTENTS

Published by
THE CHEMICAL INSTITUTE OF CANADA
OTTAWA CANADA

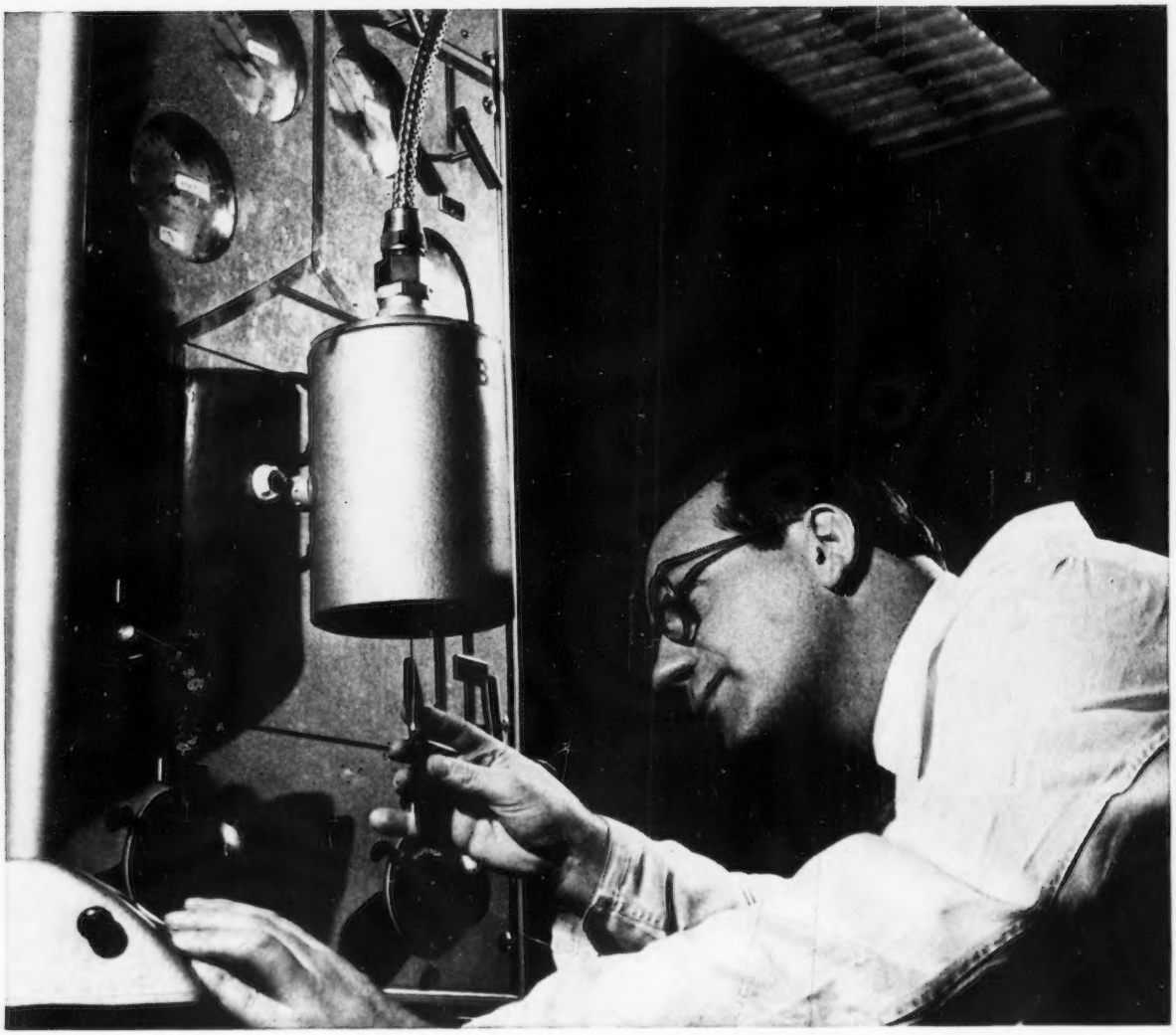

Photograph taken at C-I-L Central Research Laboratory, McMasterville, Que.

Plastics Detective

This photograph shows the High Shear Viscometer, designed and built at our Central Research Laboratory, used to investigate factors involved in complex flow behaviour of molten thermo-plastics during commercial processing.

Information on this newly developed pressure-driven capillary Viscometer has been made available to industry by C-I-L, and many industrial laboratories in the United States, England, India and Australia have built identical machines.

Such C-I-L research contributes to higher standards of performance in the plastics industry, to new and better plastics products and—through better technical service—to greater success in the application of these new materials to modern living.

C-I-L **CANADIAN INDUSTRIES LIMITED**

Serving Canadians Through Chemistry

Agricultural Chemicals • Ammunition • Coated Fabrics – Industrial Chemicals • Commercial Explosives • Paints • Plastics • Textile Fibres

The Canadian Journal of Chemical Engineering

formerly

Canadian Journal of Technology

VOLUME 38 | FEBRUARY, 1960 | NUMBER 1

Authorized as second class mail, Post Office Department, Ottawa. Printed in Canada

Manuscripts for publication should be submitted to the Editor: Dr. A. Cholette, Faculty of Science, Laval University, Boulevard de l'Entente, Quebec, Que. (Instructions to authors are on the next page).

Editorial, Production and Circulation Offices: 48 Rideau Street, Ottawa 2, Ont.

Advertising Office: C. N. McCuaig, manager of advertising sales, *The Canadian Journal of Chemical Engineering*, Room 601, 217 Bay Street, Toronto, Ont. Telephone—EMpire 3-3871.

Plates and Advertising Copy: Send to *The Canadian Journal of Chemical Engineering*, 48 Rideau Street, Ottawa 2, Ont.

Subscription Rates: In Canada—$3.00 per year and 75c per single copy; U.S. and U.K.—$4.00; Foreign—$4.50.

Change of Address: Advise Circulation Department in advance of change of address, providing old as well as new address. Enclose address label if possible.

The Canadian Journal of Chemical Engineering is published by The Chemical Institute of Canada every two months.

The Canadian Journal of Chemical Engineering

INSTRUCTIONS TO AUTHORS

Manuscript Requirements for Articles

1. The manuscript should be in English or French.
2. The original and two copies of the manuscript should be supplied. These are to be on 8½ x 11 inch sheets, typewritten, and double spaced. Each page should be numbered.
3. Symbols should conform to American Standards Association. An abridged set of acceptable symbols is found in the third edition of Perry's Chemical Engineers' Handbook. Greek letters and subscripts and superscripts should be carefully made.
4. Abstracts of not more than 200 words in English indicating the scope of the work and the principal findings should accompany all technical papers.
5. References should be listed in the order in which they occur in the paper, after the text, using the form shown here: "Othmer, D. F., Jacobs, Jr., J. J., and Levy, J. F., Ind. Eng. Chem. **34**, 286 (1942). Abbreviations of journal names should conform to the "List of Periodicals Abstracted by Chemical Abstracts". Abbreviations of the common journals are to be found in Perry's Handbook also. All references should be carefully checked with the original article.
6. Tables should be numbered in Arabic numerals. They should have brief descriptive titles and should be appended to the paper. Column headings should be brief. Tables should contain a minimum of descriptive material.
7. All figures should be numbered from 1 up, in Arabic numerals. Drawings should be carefully made with India ink on white drawing paper or tracing linen. All lines should be of sufficient thickness to reproduce well, especially if the figure is to be reduced. Letters and numerals should be carefully and neatly made, with a stencil. Generally speaking, originals should not be more than twice the size of the desired reproduction; final engravings being 3¼ in. or 7 in. wide depending on whether one column or two is used.
8. Photographs should be made on glossy paper with strong contrasts. Photographs or groups of photographs should not be larger than three times the size of the desired reproduction.
9. All tables and figures should be referred to in the text.

Submission of Manuscripts

1. The three copies of the manuscript, including figures and tables, should be sent directly to:
   DR. A. CHOLETTE, editor,
   The Canadian Journal of Chemical Engineering,
   Faculty of Science, Laval University,
   Boulevard de l'Entente,
   Quebec, Que.
2. The authors addresses and titles should be submitted with the manuscript.
3. The author may suggest names of reviewers for his article, but the selection of the reviewers will be the responsibility of the editor. Each paper or article is to be reviewed by two chemical engineers familiar with the topic. Reviewers will remain anonymous.
4. All correspondence regarding reviews should be directed to the editor.

Reprints

1. At least 50 free "tear sheets" of each paper will be supplied.
2. Additional reprints may be purchased at cost. An estimated cost of reprints, with an attached order form, will be sent to the author with the galley proofs.
3. Orders for reprints must be made before the paper has appeared in the Journal.

Communications, Letters and Notes to the Editor

Short papers, as described below, will be considered for publication in this Journal. Their total length should not exceed 600 words, or its equivalent.

Communications

A communication is a prompt preliminary report of observations made which are judged to be sufficiently important to warrant expedited publication. It usually calls for a more expanded paper in which the original matter is republished with more details.

Letters

A letter consists of comments or remarks submitted by readers or authors in connection with previously published material. It may deal with various forms of discussion arising out of a publication or it may simply report and correct inadvertent errors.

Notes

A note is a short paper which describes a piece of work not sufficiently important or complete to make it worth a full article. It may refer to a study or piece of research which, while it is not finished and may not be finished, offers interesting aspects or facts. As in the case of an article a note is a final publication.

* * *

Performance of Flow Reactors at Various Levels of Mixing[1]

A. CHOLETTE[2], J. BLANCHET[2] and LÉONCE CLOUTIER[2]

Chemical flow reactors studied include models in which partial mixing and piston flow are present and others which involve partial mixing and short-circuit. Mixing levels considered extend all the way between the extreme cases of tubular and continuous-stirred tank reactors. Various orders of reaction are taken into account.

The curves presented, obtained through analytical methods, show either the variation of conversion with mixing level at given values of residence time, or relative residence times for a given conversion.

Graphical methods of solution are proposed. They involve, in part, a means of computation whereby the overall conversion for a number of reactors in series is obtained from the individual conversions.

While isothermal conditions only have been considered, more interesting results are expected when other conditions are applicable, whether isothermal or not.

Les auteurs étudient des réacteurs chimiques à régime continu comprenant des modèles où on trouve tantôt l'agitation partielle et l'écoulement frontal, tantôt l'agitation partielle et le court-circuit. Ils considèrent des niveaux d'agitation variant entre les cas extrêmes de réacteurs tubulaires et de réacteurs parfaitement agités. Ils présentent les résultats se rapportant à différents ordres de réaction.

On obtient par méthodes analytiques des courbes qui montrent, soit la variation de la conversion avec le niveau d'agitation pour un temps de séjour donné, soit les temps de séjour relatifs pour une conversion donnée.

Les auteurs proposent des méthodes de solutions graphiques. Elles comportent, en partie, une façon de calculer la conversion totale, pour des réacteurs en série, à partir des conversions individuelles.

On ne considère dans le présent travail que des conditions isothermiques, mais on prévoit aussi des résultats intéressants pour d'autres conditions, isothermiques ou non.

DESIGN procedures pertaining to chemical flow reactors are readily available for relatively simple models [1], such as tubular or continuous-stirred-tank reactors (CSTR).

Flow patterns in such reactors correspond to limiting cases. While CSTR's can easily be realized, tubular reactors seldom meet perfectly the assumption of true plug flow.

Actual reactors will often perform in such a way that results lie between those predicted for tubular and CST reactors [2, 3].

Various methods of approach have been suggested to deal with departures from ideal conditions. Residence time studies have been the object of considerable work [2, 4, 5, 6, 7], but do not account for a complete solution. Different techniques have been used in such work, some involving radioactive tracers [3, 5, 6, 8, 9, 10]. Other investigators have worked along the concept of partial backmixing or intermixing [2, 11, 12, 13, 14, 15, 16]. Thus, some have compared an actual reactor to the equivalent number of CSTR in series giving the same results.

More recent studies were aimed at analyzing reactor performance through the introduction of diffusivity, involving Peclet number [17, 18, 19, 20, 21].

In a recent study by Cholette and Cloutier [22], on the efficiency of mixing in continuous flow systems, different models have been presented in which various combinations of piston flow, effective volume of mixing and short-circuit were discussed. The case of chemical reactors was introduced and, as indicated, was to be expanded.

The present study deals with models in which partial mixing and piston flow exist and others where partial mixing and short-circuiting take place.

Before investigating such reactors, it is useful to review briefly the extreme cases: the tubular reactor where no mixing is present and the CSTR which exhibits perfect mixing.

Design procedures rely deeply upon reaction rates. These involve a number of variables [23] and can be expressed in different ways [24]. One of the main factors is temperature, as heat effects can play an important role in the design of a reactor.

While only isothermal conditions have been considered in the present study, the scope of the latter is not limited to that case alone. Endothermic or exothermic reactions resulting in non-isothermal conditions can be studied as well and will be the subject of a future publication.

TUBULAR REACTORS

Design equations available for tubular reactors, applied to a model such as shown in Figure 1, give the following expression, when the density in a liquid system, or the number of moles in a gaseous system, is assumed constant:

[1]*Manuscript received September 25; accepted November 20, 1959.*

[2]*Université Laval, Quebec, Que.*

Contribution from the Chemical Engineering Department, Université Laval, Quebec, Que. and presented at the C.I.C. Chemical Engineering Conference, Hamilton, Ont., November 9-11, 1959.

$$\left(\frac{V}{q}\right)_i = \theta_i = -\int_{C_F}^{C_i} \frac{dC}{r} \quad \ldots\ldots(1)$$

One Reactant

Of the many ways in which to express the reaction rate, the usual one for homogeneous irreversible reactions is:

$$r = k\,C^a \quad \ldots\ldots(2)$$

where a is the order of the reaction. Usually, the velocity rate constant k is known or can be calculated [1, 24, 25].

For a first-order reaction, integration of Equation (1) gives:

$$\theta_i = \frac{1}{k}\,ln\;C_F/C_i \quad \ldots\ldots(3)$$

Introducing x, the degree of conversion as defined in Smith [1], (MacMullin and Weber [26] and Eldridge and Piret [27] used the symbol D), the feed and effluent concentrations in any flow system are related as follows:

$$x = \frac{C_F - C_E}{C_F} \quad \text{or} \quad C_F/C_E = \frac{1}{1-x} \quad \ldots\ldots(4)$$

Equation (3) can thus be written:

$$\theta_i = \frac{1}{k}\,ln\,\frac{1}{1-x_i} \quad \ldots\ldots(5)$$

a plot of which appears in Figure 2. From this graph, the residence time or conversion can be obtained directly.

For a second-order reaction, $r = k\,C^2$ and Equation (1) yields:

$$C_F k\theta_i = \frac{x_i}{1-x_i} \quad \ldots\ldots(6)$$

When plotted as in Figure 3 it is convenient for determining either the residence time or the conversion. Other combinations are also possible.

For third-order reactions, $r = k\,C^3$ and the design equation is:

$$C_F^2 k\theta_i = \frac{(1 - 0.5\,x_i)x_i}{(1-x_i)^2} \quad \ldots\ldots(7)$$

It is convenient to use when plotted as in Figure 4.

Figures 2, 3 and 4 can be useful when evaluating the ratios θ/θ_i or V/V_i in dealing with partial mixing, as has been done in later sections. Integration of Equation (1) gives the following general expression for all values of a except unity (in which case Equation (5) applies):

$$\theta_i = \frac{1}{k(a-1)}\,(C_i^{1-a} - C_F^{1-a}) \quad \ldots\ldots(8)$$

Two Reactants

Second-order reactions are often those which result from the interaction of two components. For reactions of the type

$$A + B \rightarrow \text{products}$$

the reaction rate is:

$$r = k\,C_A C_B$$

For the study of these reactions it is often convenient to define the ratio:

$$R = \frac{C_{B_F}}{C_{A_F}} \text{ where } C_{B_F} > C_{A_F}$$

In this case, the degree of conversion x refers to the limiting reactant, that in lesser concentration.

Integration of Equation (1) gives in this case:

$$C_{A_F}\,k\,\theta_i = \frac{1}{R-1}\,ln\,\frac{R - x_i}{R(1-x_i)} \quad \ldots\ldots(9)$$

When $R = 1$, the case reverts to one of a second-order reaction with one reactant, and Equation (6) applies.

Curves showing the variation of $C_{A_F}\,k\theta_i$ with x, at different values of R, are presented by Caddell and Hurt [28] and by Lessels [11].

These authors, as well as Jenney [29] and Nord [30], also present nomographs relating to Equations (5), (6), (7) and (9). While they serve a similar purpose as Figures 2, 3, 4, they do not apply in the same way and are less convenient for some phases of the present work.

When deriving the preceding expressions for tubular reactors, true plug flow is assumed. In practice, such conditions are seldom attained. A study of the effect of turbulent and laminar flow in reactors was presented by Bosworth [31]. Denbigh [32] reports that while turbulent flow approximates closely the hypothesis of true plug flow, laminar flow does not.

As indicated by the latter [32, 33], and also by Greenhalgh [14] and Gorrigan and Young [12], correlations obtained for tubular reactors are also applicable to batch reactors when the residence time in the former is the same as the reaction time of the latter.

A tubular reactor can be considered as made up of an infinite number of infinitely small batch reactors [14] or continuous-flow stirred-tank reactors in series [26], of the same total volume.

CONTINUOUS-FLOW STIRRED-TANK REACTORS (CSTR)

In an ideal CSTR, as in Figure 5, there is uniformity of composition and temperature throughout the reactor. The concentration of the outlet stream is then the same as that in the reactor. Other pertinent assumptions [15] are applicable.

Many design equations are available, but the basic CSTR equation may be written as follows [1]:

$$C_F - C_M = r_M\theta_M \quad \ldots\ldots(10)$$

One Reactant

In general, the reaction rate for an homogeneous, irreversible reaction is given by:

$$r_M = k\,C_M^a \quad \ldots\ldots(11)$$

Some investigators [34, 35] have found it convenient to use this simple expression to determine experimentally the velocity rate constant, k.

Combining Equations (10) and (11), one obtains:

(a) for a first-order reaction

$$k\,\theta_M = \frac{x_M}{1-x_M} \quad \ldots\ldots(12)$$

(b) for a second-order reaction

$$C_F\,k\,\theta_M = \frac{x_M}{(1-x_M)^2} \quad \ldots\ldots(13)$$

(c) for a third order reaction

$$C_F^2 k\,\theta_M = \frac{x_M}{(1-x_M)^3} \quad \ldots\ldots(14)$$

While not presented here, graphs obtained from these three equations are similar in form to those presented for tubular reactors in Figures 2, 3 and 4 and can be just as useful.

Two Reactants

In the case of a second-order reaction the rate can be expressed as follows:

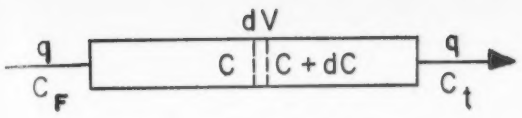

Figure 1—Tubular reactor.

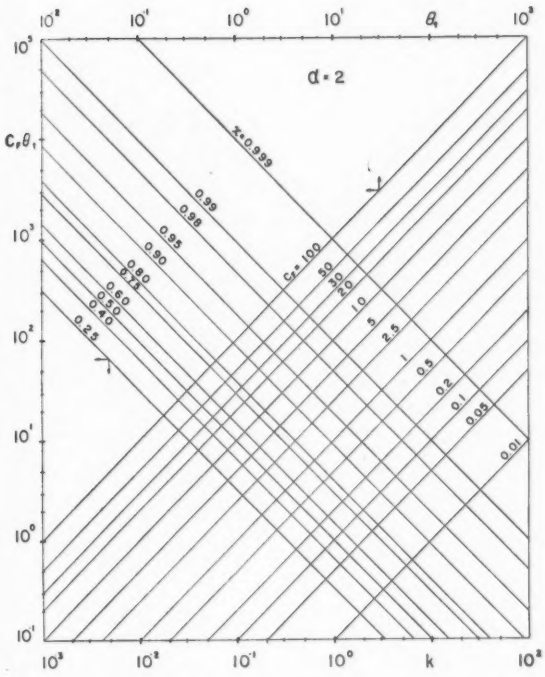

Figure 3 Graphical determination of variables in tubular reactors, second-order reactions.

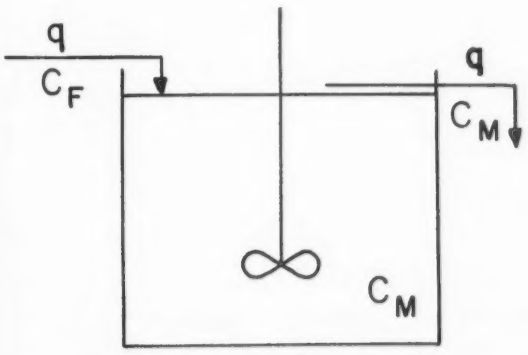

Figure 5—Continuous-stirred-tank reactor (CSTR).

$$r_M = k\, C_{A_M}\, C_{B_M}$$

The design equation obtained from Equation (10) is then:

$$C_{A_F}\, k\, \theta_M = \frac{x_M}{(1 - x_M)\,(R - x_M)} \qquad \ldots\ldots\ldots\ldots (15)$$

For equimolar concentrations, this equation reverts to Equation (13).

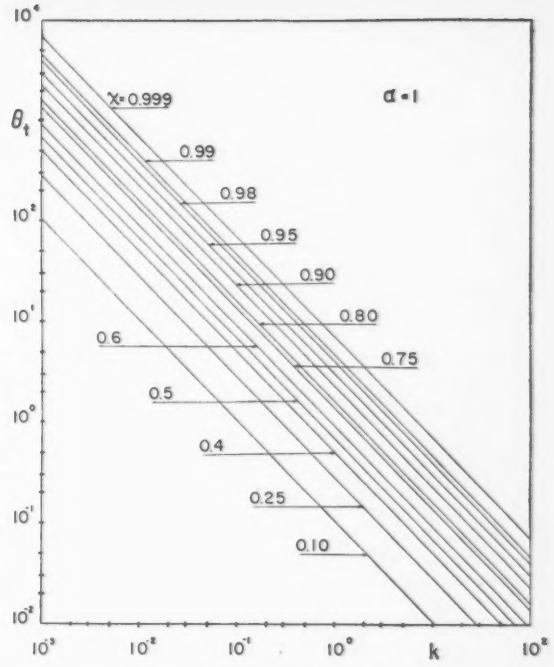

Figure 2—Graphical determination of variables in tubular reactors, first-order reactions.

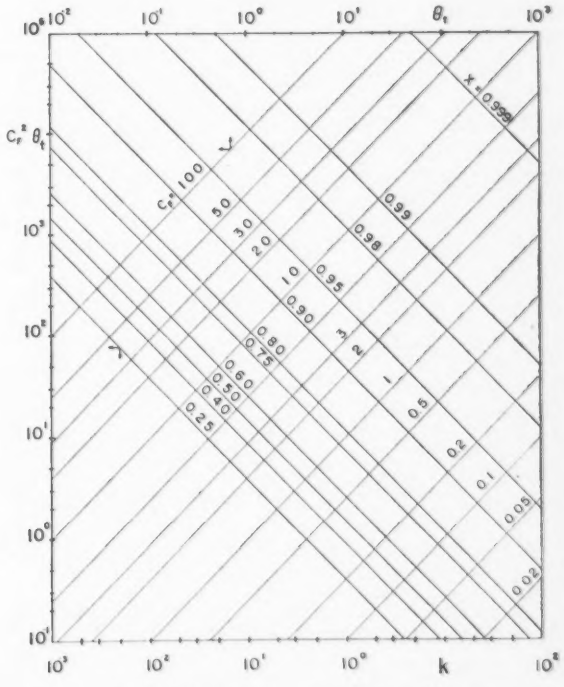

Figure 4 Graphical determination of variables in tubular reactors, third-order reactions.

Graphs relating to first and second-order reactions in CSTR are presented by Lessels [11] and Jenney [29].

COMPARISON OF TUBULAR AND CST REACTORS

As pointed out by Reman [36], tubular and CST reactors can be compared in two ways:

(a) the conversions obtained for a given residence time.

(b) the residence times or volumes required to achieve a given conversion.

The latter case has been the subject of several studies [2, 11, 12, 26, 36, 37] which do not need to be extended for the present work.

As for the conversions obtained for a given residence time, a simple relation can be derived from Equations (8), (10) and (11), in the case of one reactant, noting that $\theta_M = \theta_t$

$$\frac{C_F - C_M}{C_M^a} = \frac{1}{a - 1}\left(C_t^{1-a} - C_F^{1-a}\right) \quad \ldots\ldots(16)$$

which can be rewritten in the following form:

$$x_t = 1 - \left[1 + (a - 1)\frac{x_M}{(1 - x_M)^a}\right]^{\frac{1}{1-a}} \quad \ldots\ldots(17)$$

This expression is a general one for all values of a except unity. In this case,

$$x_t = 1 - e^{-\frac{x_M}{1-x_M}} \quad \ldots\ldots(18)$$

Plots of Equations (17) and (18) are shown in Figure 6. Some of these have already been given by Reman [36]. Similar curves can be presented for any value of a; those for $a = 0.5$, 0.75 and 1.5 have been calculated but were not included in Figure 6 to prevent overcrowding.

It is interesting to note the variation of x_t/x_M as a function of x_t, in Figure 7, for isothermal conditions. A limited graph of the inverse ratio x_M/x_t has been presented by Corrigan and Young [12], as a function of x_t, for a second-order reaction.

While the ratio x_t/x_M is close to unity at low and high values of conversions, it reaches a maximum at intermediate values. Although for the reactions under consideration in the present work a tubular reactor is always more effective than a CSTR of equal residence time or volume, it is decidedly more so in the region where the values of x_t/x_M go through a maximum in the curves of Figure 7. It may be noticed that the particular value of the conversion at which the maximum occurs shifts with the order of reaction. For each order of reaction the maximum can be read directly on the curves of Figure 7 or it can be calculated by dividing Equation (17) by x_M, and setting $\frac{d(x_t/x_M)}{d\,x_M} = 0$. A plot of $(x_t/x_M)_{max}$ as a function of a is shown in Figure 8, along with the corresponding values of x_t and x_M.

Since the conditions for which Figure 8 applies are met only in particular cases, another comparison of the relative performance of the two reactors can be made by showing the variation of x_t/x_M as a function of a for given values of the conversion x_t, as in Figure 9.

It may be seen from this figure that the relative advantage of the tubular reactor over the CSTR is more pronounced at intermediate conversions for the usual reaction orders, 1 and 2. Except at low conversions, the tubular reactor always has a decided advantage over the CSTR for first-order reactions.

CONTINUOUS FLOW REACTORS WITH PARTIAL MIXING

Of the models defined by Cholette and Cloutier [22], only the following are considered in the present work:

(A) Partial Mixing and Piston Flow.

In such a model, a fraction m of the reactor contents is assumed to be perfectly mixed while the other, $(1 - m)$, travels in piston flow. Within this model, many combinations are possible depending on the location of the well-mixed zone. The limiting cases considered are as described below and both analytical and graphical methods are presented for their solution. A comparison of the two models is also made.

(a) Model TM.

As shown in Figure 10(a), the flow in this model is such that the reactants first undergo piston flow and then pass through a zone of perfect mixing.

(b) Model MT.

Figure 11(a) shows that the reactants enter a zone of perfect mixing and then pass into one of piston flow.

(B) Partial Mixing and Short-circuiting.

The flow pattern and mixing characteristics are as shown in Figure 12. This model has been discussed briefly [22] for zero-order reactions and for first-order reactions when no short-circuiting is present. It is studied more extensively and in a general way in the present article.

A. Partial Mixing and Piston Flow.

a) Model TM

1. *Conversions obtained for a given residence time.*

The flow through the reactor, Figure 10(a) is such that the reactants first undergo tubular or plug flow and then enter a zone of perfect mixing, of volume mV. The residence time, $\frac{(1-m)V}{q}$, for the tubular section, is assumed to be the same for all elements.

Such a model would behave like a tubular reactor of volume $(1 - m)\ V$ followed immediately by a CSTR of volume mV, as shown in Figure 10(b). A similar arrangement is discussed in a recent paper by Zwietering [38].

Referring to Figure 10 and applying Equation (1), the results for the tubular part of the reactor are:

$$(1 - m)\frac{V}{q} = -\int_{C_F}^{C_t} \frac{dC}{r_t} \quad \ldots\ldots(19)$$

For the zone of perfect mixing, applying Equation (10), gives:

$$C_t - C_E = \frac{r'\,m\,V}{q} \quad \ldots\ldots(20)$$

The performance of such a reactor can then be obtained by combining Equations (19 and 20) and comparing the results with those that would be obtained with a tubular reactor of equal residence time, as given by Equation (1), C_t being the theoretical outlet concentration for tubular flow.

Combining Equations (1) and (20) gives:

$$C_t = C_E - r'\,m\int_{C_F}^{C_t} \frac{dC}{r} \quad \ldots\ldots(21)$$

which, when introduced into Equation (19), leads to the general expression:

$$\int_{C_F}^{C_E - r'\,m\int_{C_F}^{C_t}\frac{dC}{r}} \frac{dC}{r_t} = (1 - m)\int_{C_F}^{C_t}\frac{dC}{r} \quad \ldots\ldots(22)$$

For a first-order, irreversible, homogeneous reaction, Equation (22) simplifies to:

$$C_F/C_E = \left(1 + m\ ln\ \frac{C_F}{C_t}\right)\left(\frac{C_F}{C_t}\right)^{1-m} \quad \ldots\ldots(23)$$

or, in terms of conversion:

$$x = 1 - \frac{(1 - x_t)^{1-m}}{1 - ln\,(1 - x_t)^m} \quad \ldots\ldots(24)$$

Curves showing the variation of x with m are given in Figure 13, at values of $(V/q)_t$ corresponding to a number of conversions x_t. As the residence time increases, giving larger values of x_t,

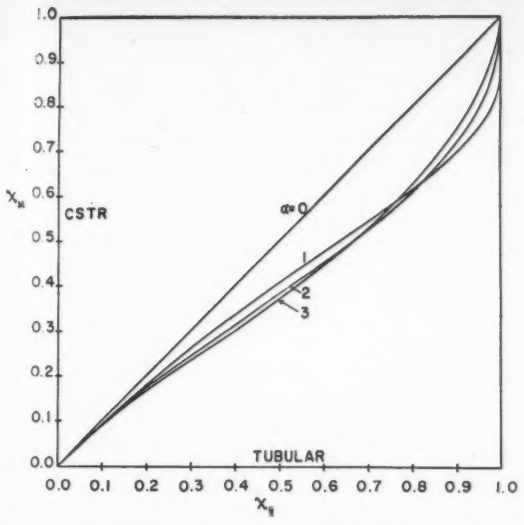

Figure 6—Conversion in a tubular reactor compared to that in a CSTR of equal residence time, for various orders of reaction.

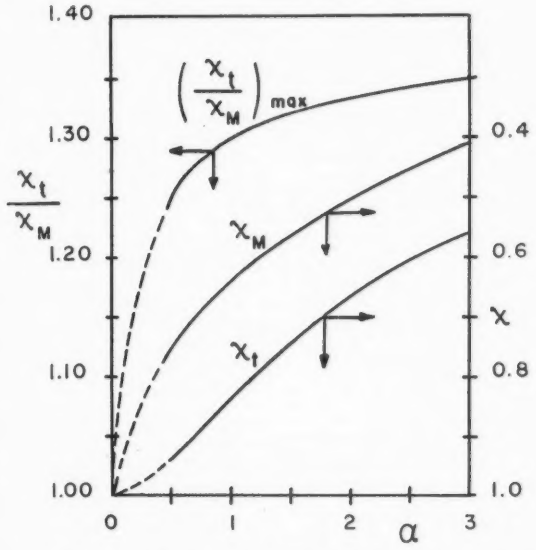

Figure 8—Variation of the maximum value of the ratio x_t/x_M as a function of the order of reaction.

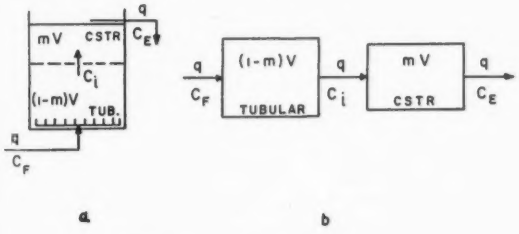

Figure 10—Description of Model TM.

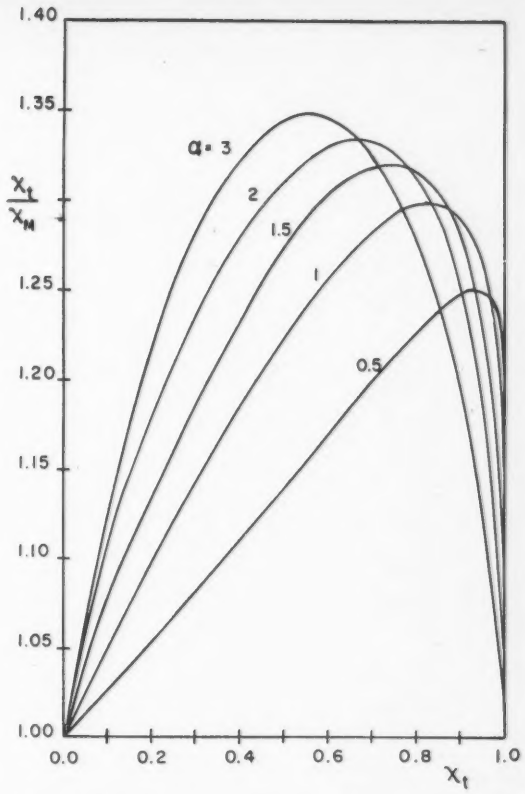

Figure 7—Variation of the relative conversion x_t/x_M, for reactors of equal residence time, as a function of the conversion in a tubular reactor.

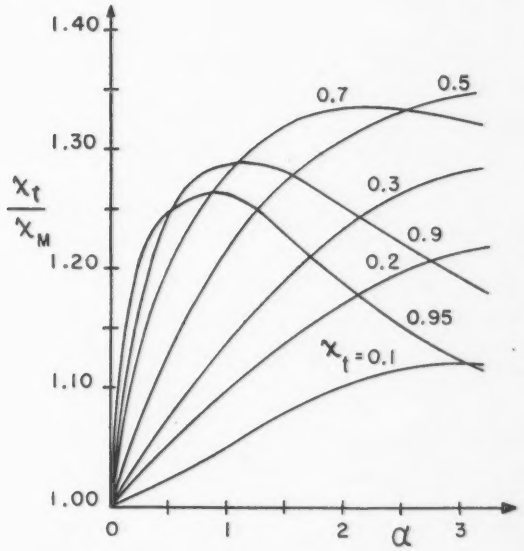

Figure 9—Variation of the relative conversion x_t, x_M as a function of the order of reaction, at given values of x_t.

the conversion is less and less affected by the degree of mixing, especially at low values of m.

In a second-order reaction, when one reactant is present, Equation (22) gives:

$$m = \frac{(C_F/C_i - C_F/C_E) + \sqrt{(C_F/C_i - C_F/C_E)^2 + 4\,C_F/C_E(C_F/C_i - C_F/C_E)}}{2\,(C_F/C_i - 1)} \quad \ldots\ldots(25)$$

or, in terms of conversion:

$$m = \frac{x_t - x}{2x_t(1-x)}\left[1 + \sqrt{1 + 4\,\frac{1-x_t}{x_t - x}}\right] \quad \ldots\ldots(26)$$

Figure 14 shows the variation of x with m in this case for given values of x_t.

If two reactants in unequivalent molar amount undergo a

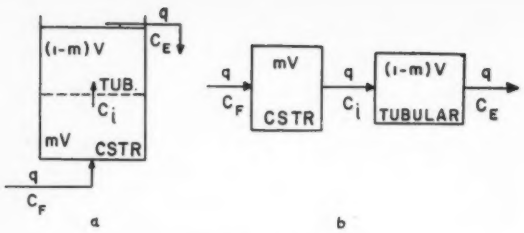

Figure 11—Description of Model MT.

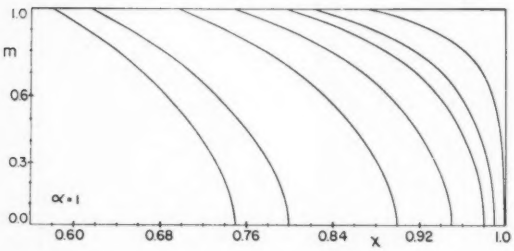

Figure 13—Variation of the conversion with m, for first-order reactions, applicable to Models TM and MT. Each curve corresponds to a residence time such that the conversion in a tubular reactor is read at $m = 0$.

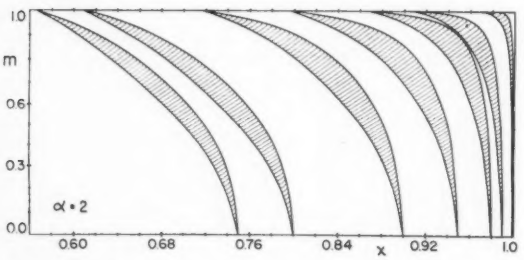

Figure 14—Variation of the conversion with m, for second-order reactions. Each set of curves corresponds to a residence time such that the conversion in a tubular reactor is read at $m = 0$. The upper curve of each set is for Model TM reactors, while the lower curve is for Model MT.

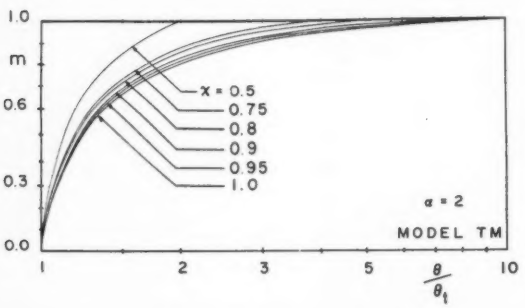

Figure 16—Variation of relative residence times with m, in Model TM, for second-order reactions, at the conversions indicated on each curve.

second-order reaction, the following expression is derived from Equation (22):

$$(1 - x)\left[(R - 1) + (R - x)\,ln\left(\frac{R - x_t}{R(1 - x_t)}\right)^m\right] = \frac{(R - 1)^2}{R\left(\frac{(R - x_t)}{R(1 - x_t)}\right)^{1-m} - 1} \quad \ldots\ldots (27)$$

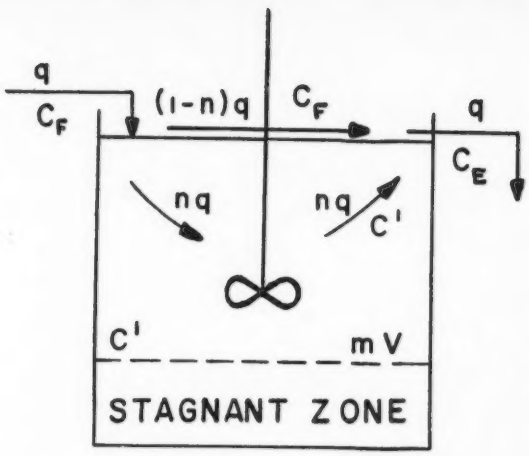

Figure 12—Description of a reactor where partial mixing and short-circuit take place.

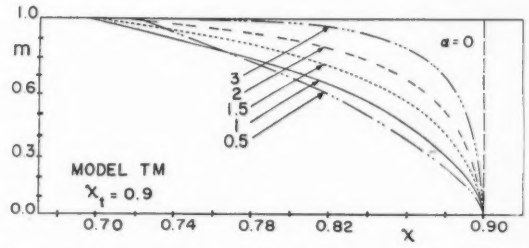

Figure 15—Variation of x with m, in Model TM, for different orders of reaction. The residence time is such that the conversion in a tubular reactor would be 90%.

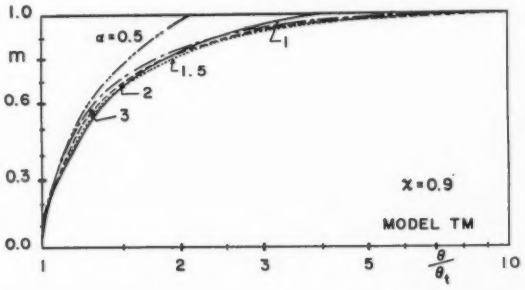

Figure 17—Variation of relative residence times with m, in Model TM, for different orders of reaction, at a fixed conversion of 90%.

As might be expected, an examination of this expression shows that $x = x_t$ when $m = 0$, and that $x = x_M$ when $m = 1$. This is confirmed by inspection of Equations (9) and (15) for $\theta_t = \theta_M$.

When the two reactants are present in equimolar concentrations, $R = 1$ and Equation (26) applies.

A graph can be made from Equation (27), presenting families of curves showing the variation of x with m, at given values of x_t and R. Applying Equation (22) to reactions of order 0.5, 1.5 and 3, the following expressions are derived:

For $\alpha = 0.5$

$$m = \frac{[(C_F/C_t)^{0.5} - (C_F/C_E)^{0.5}] + \sqrt{[(C_F/C_t)^{0.5} - (C_F/C_E)^{0.5}]^2 + [C_F/C_t - C_F/C_E]}}{(C_F/C_E)^{0.5}[(C_F/C_t)^{0.5} - 1]} \quad \ldots\ldots(28)$$

For $\alpha = 1.5$:

$$m^3 - \left[\frac{4(C_F/C_t)^{0.5} - (C_F/C_E)^{0.5}}{2[(C_F/C_t)^{0.5} - 1]}\right] m^2 + \left[\frac{(C_F/C_t)^{0.5}[(C_F/C_t)^{0.5} - (C_F/C_E)^{0.5}]}{[(C_F/C_t)^{0.5} - 1]^2}\right] m + \left[\frac{(C_F/C_E)^{0.5}(C_F/C_t - C_F/C_E)}{2[(C_F/C_t)^{0.5} - 1]^3}\right] = O \ldots.(29)$$

For $\alpha = 3$:

$$m^3 - \left[\frac{4[0.25(C_F/C_t)^2 - (C_F/C_E)^2]}{(C_F/C_t)^2 - 1}\right] m^2 - \left[\frac{4(C_F/C_E)^2[(C_F/C_t)^2 - (C_F/C_E)^2]}{[(C_F/C_t)^2 - 1]^2}\right] m - \left[\frac{4(C_F/C_E)^4[(C_F/C_t)^2 - (C_F/C_E)^2]}{[(C_F/C_t)^2 - 1]^3}\right] = O \ldots.(30)$$

For values of C_F, C_t and C_E, corresponding to a given conversion, m is obtained by successive approximations.

Application of Equation (22) to a zero-order reaction shows that $x = x_t$ irrespective of the values of m, and the degree of conversion depends only on the residence time.

For a residence time such that the conversion x_t in a tubular reactor would be 0.9, figure (15) shows the variation of conversion with m for the above cases. It may be observed that as conditions depart from those of a tubular reactor, the conversion is less and less affected by the extent of mixing as the order of reaction increases from a value of 0.5; although no curves are presented for very low orders of reaction, the opposite effect would be noticed as α varies from 0 to 0.5.

2. *Residence times or volumes required for a given conversion.*

For the tubular section of the TM reactor shown in Figure (10), the following equation holds:

$$-\int_{C_F}^{C_t} \frac{dC}{C^\alpha} = (1 - m)k\theta \quad \ldots\ldots(31)$$

which, upon integration for $\alpha \neq 1$ gives:

$$(1 - m)k\theta = \frac{1}{\alpha - 1}(C_t^{1-\alpha} - C_F^{1-\alpha}) \quad \ldots\ldots(32)$$

As the reaction takes place thereafter in a zone of perfect mixing, one obtains:

$$\frac{C_i - C_E}{C_E^\alpha} = mk\theta \quad \ldots\ldots(33)$$

which can be transformed to:

$$C_i = C_E + m\,C_E^\alpha\,k\theta \quad \ldots\ldots(34)$$

Combining Equations (32) and (34) yields:

$$C_E^{1-\alpha}[1 + m\,C_E^{\alpha-1}(k\theta)]^{1-\alpha} = C_F^{1-\alpha} + (\alpha - 1)(1 - m)\,k\theta \ldots(35)$$

valid for reaction orders other than one.

If plug flow prevailed throughout the above reactor, the feed and effluent concentrations would be related by the following equation, where $\alpha \neq 1$:

$$k\theta_t = \frac{1}{\alpha - 1}(C_t^{1-\alpha} - C_F^{1-\alpha}) \quad \ldots\ldots(36)$$

The ratio of residence times θ/θ_t or that of the volumes V/V_t is obtained as follows for identical conversions in the two reactors under consideration:

$$\frac{\theta}{\theta_t} = \left(\frac{V}{V_t}\right)_q = \frac{(k\theta)_{\text{Eq. 35}}}{(k\theta_t)_{\text{Eq. 36}}} \quad \ldots\ldots(37)$$

In a zero-order reaction, consideration of Equations (35), (36) and (37) shows that $\theta/\theta_t = 1$ for all values of m.

For a second-order reaction, Equations (35), (36) and (37) give:

$$\frac{\theta}{\theta_t} = \frac{\sqrt{(1 - mx)^2 + 4m(1 - m)x} - (1 - mx)}{2m(1 - m)x} \quad \ldots\ldots(38)$$

wherein m is different from zero or unity.

Curves showing the variation of θ/θ_t with m, at different conversions, are given in Figure (16). As the conversion increases, the relative residence times increase more and more rapidly when the degree of mixing approaches unity.

When two reactants undergoing a second-order chemical reaction are present in unequivalent molar concentrations, the following expression applies:

$$\left[\frac{1 + m(1 - x)(C_{A_F}k\theta)}{1 + m(R - x)(C_{A_F}k\theta)}\right]\left[\frac{R - x}{R(1 - x)}\right] = e^{(R-1)(1-m)(C_{A_F}k\theta)} \quad \ldots\ldots(39)$$

The ratio θ/θ_t is then obtained as follows:

$$\frac{\theta}{\theta_t} = \frac{[C_{A_F}k\theta]_{\text{Eq. 39}}}{[C_{A_F}k\theta_t]_{\text{Eq. 9}}} = \frac{[C_{A_F}k\theta]_{\text{Eq. 39}}}{\frac{1}{R-1}\ln\frac{R - x}{R(1 - x)}} \quad \ldots\ldots(40)$$

Many families of curves can be obtained from Equation (40), depending upon the values of the different parameters contained. Only the particular case of equimolar concentrations is considered here, as Equation (40) reverts to Equation (38) when $R = 1$. Curves for this particular case are shown in Figure (16).

When $\alpha = 0.5$, Equations (35), (36) and (37) yield:

$$\frac{\theta}{\theta_t} = \frac{\left[(1-m)\sqrt{\frac{C_F}{C_E}} + m\right] - \sqrt{\left[(1-m)\sqrt{\frac{C_F}{C_E}} + m\right]^2 - (1-m)^2\left(\frac{C_F}{C_E} - 1\right)}}{(1-m)^2(\sqrt{C_F/C_E} - 1)} \quad \ldots\ldots(41)$$

in which m must be different from unity.

For $\alpha = 1.5$, Equation (35) becomes:

$$(k\theta)^3 + \left[\frac{4[m(C_E/C_F)^{0.5} + 0.25(1 - m)]}{m(1 - m)\,C_E^{0.5}}\right](k\theta)^2 + \left[\frac{4[m(C_E/C_F)^{0.5} + (1 - m)]}{m(1 - m)^2 C_F^{0.5} C_E^{0.5}}\right]k\theta - \frac{4(1 - C_E/C_F)}{m(1 - m)^2 C_E^{1.5}} = O \ldots.(42)$$

And for $\alpha = 3$, Equation (35) gives:

$$(k\theta)^3 + \left[\frac{m(C_E/C_F)^2 + 4(1 - m)}{2m(1 - m)C_E^2}\right](k\theta)^2 + \left[\frac{m(C_E/C_F)^2 + (1 - m)}{m^2(1 - m)C_E^4}\right]k\theta - \left[\frac{(1/C_E)^2 - (1/C_F)^2}{2m^2(1 - m)C_E^4}\right] = O \ldots(43)$$

Finding values of $k\theta$ in Equations (42) and (43) by approximation and dividing by the corresponding value of $k\theta_t$ in Equation (36), gives the ratios θ/θ_t for a given conversion at different values of m.

Such curves, as well as others for different orders of reaction, are presented in Figure (17), when the conversion is 90%. Relative residence times are seen to vary rather rapidly with m, for most of the orders of reaction, as the degree of mixing approaches unity.

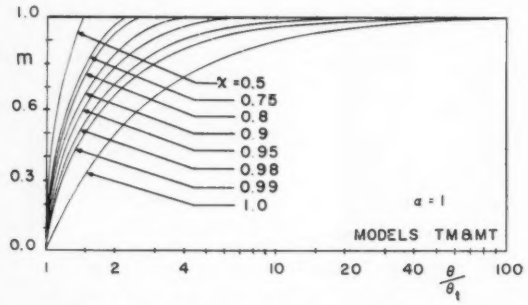

Figure 18—Variation of relative residence times with m, in Models TM and MT, for first-order reactions, at the conversion indicated on each curve.

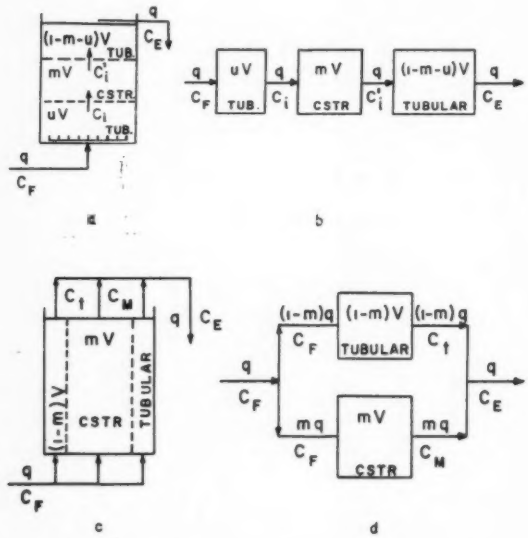

Figure 20—(a) reactor with a zone of perfect mixing located between two sections of tubular flow. (b) reactors in series, with a CSTR located between tubular reactors. (c) reactor with a zone of perfect mixing extending throughout the length of the reactor and surrounded by a section in tubular flow. (d) CSTR and tubular reactor in parallel.

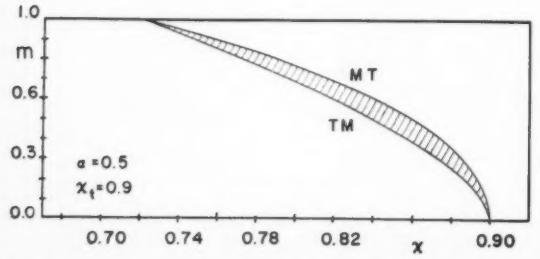

Figure 23—Comparison of the variation of conversion with m, in Models TM and MT, for $\alpha = 0.5$, at a residence time such that $x_t = 0.9$.

For the particular case of a first-order reaction, Equations (31), (33) and (34) show that the feed and effluent concentrations of the tubular section are related by:

$$ln \frac{C_F}{C_i} = (1 - m)\, k\theta \quad \ldots\ldots (44)$$

and those of the well-mixed section by:

$$\frac{C_i}{C_E} = 1 + m\, k\theta \quad \ldots\ldots (45)$$

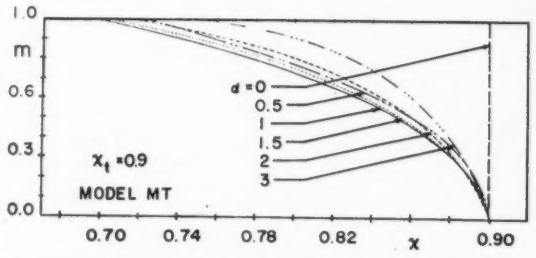

Figure 19—Variation of x with m, in Model MT, for different orders of reaction. The residence time is such that the conversion in a tubular reactor would be 90%.

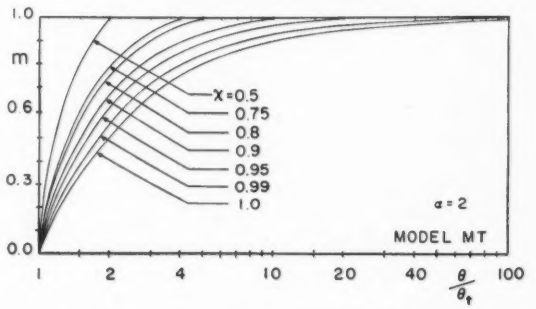

Figure 21—Variation of relative residence times with m, in Model MT, for second-order reactions, at the conversions indicated on each curve.

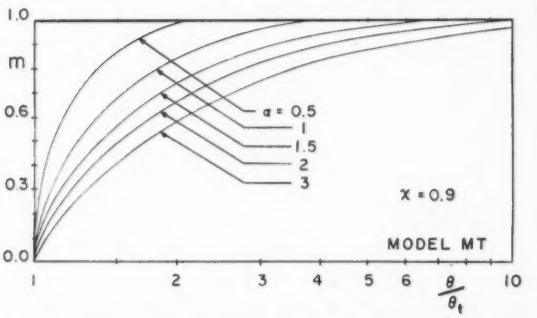

Figure 22—Variation of relative residence times with m, in Model MT, for different orders of reaction, at a given conversion of 90%.

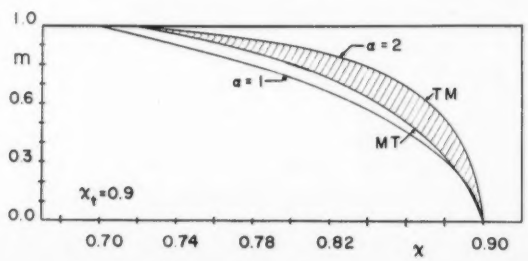

Figure 24—Comparison of the variation of conversion with m, in Models TM and MT, for first and second-order reactions, at a residence time such that $x_t = 0.9$.

Combining these two equations results in

$$\frac{C_F}{C_E} = (1 + m\,k\theta)\; e^{(1-m)\,k\theta} \qquad (46)$$

or

$$ln\,\frac{1}{1-x} = ln(1 + m\,k\theta) + (1 - m)k\theta \qquad (47)$$

From Equation (5), it is seen that, for identical values of conversion,

$$k\theta_t = ln\,\frac{1}{1-x} \qquad (48)$$

The ratio of θ/θ_t or $(V/V_t)_e$, for a first-order reaction, is thus obtained by

$$\frac{\theta}{\theta_t} = \left(\frac{V}{V_t}\right)_e = \frac{(k\theta)_{\text{Eq.47}}}{(k\theta_t)_{\text{Eq.48}}} \qquad (49)$$

As the conversion x approaches unity, the value of $k\theta$ increases rapidly and the term $ln\ (1 + m\ k\theta)$ in Equation (47) becomes negligible by comparison with $(1 - m)\ k\theta$.

The ratio of residence times or volumes for complete conversion simplifies to

$$\left(\frac{\theta}{\theta_t}\right)_{x=1} = \frac{1}{1-m} \qquad (50)$$

Curves for first-order reactions showing the variations of θ/θ_t with m at different values of conversion are shown in Figure 18. The effect of mixing on relative residence times is similar to that shown in Figure (16) for second-order reactions, except that it is more pronounced for first-order reactions.

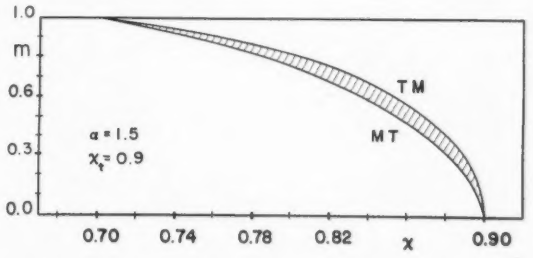

Figure 25—Comparison of the variation of conversion with m, in Models TM and MT, for $a = 1.5$, at a residence time such that $x_t = 0.9$.

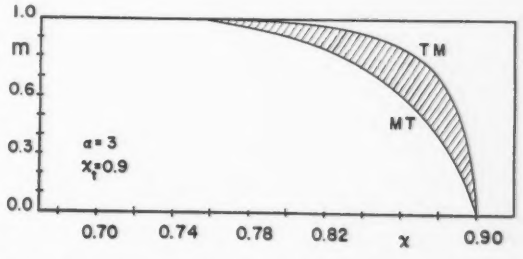

Figure 26—Comparison of the variation of conversion with m, in Models TM and MT, for $a = 3$, at a residence time such that $x_t = 0.9$.

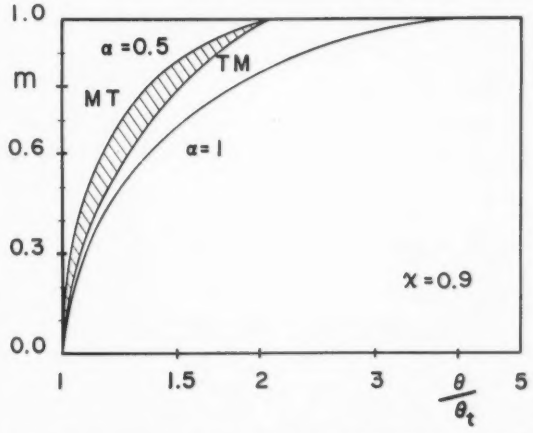

Figure 27—Comparison of the variation of relative residence times with m, in Models TM and MT, for $a = 0.5$ and $a = 1$, at a given conversion of 90%.

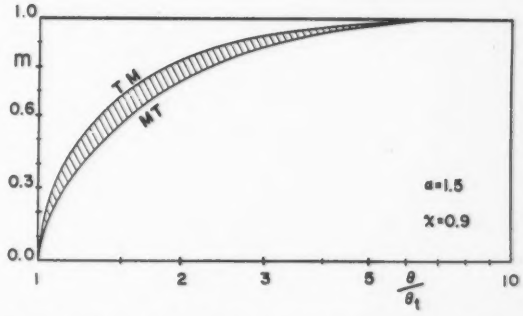

Figure 28—Comparison of the variation of relative residence times with m, in Models TM and MT, for $a = 1.5$, at a given conversion of 90%.

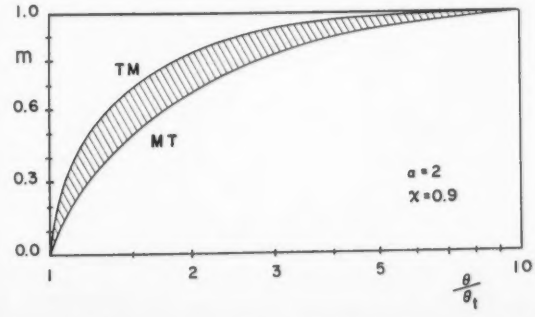

Figure 29—Comparison of the variation of relative residence times with m, in Models TM and MT, for second-order reactions, at a given conversion of 90%.

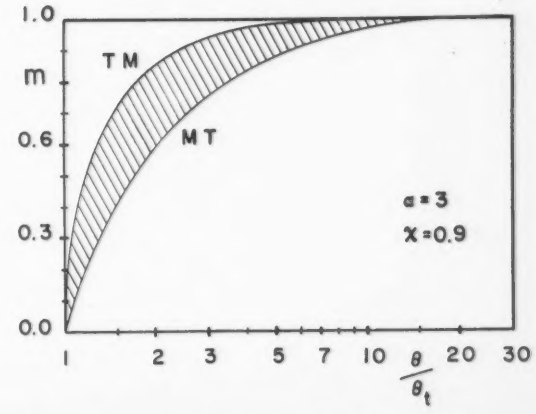

Figure 30—Comparison of the variation of relative residence times with m, in Models TM and MT, for third-order reactions, at a given conversion of 90%.

Some of the above expressions become indeterminate at $m = 1$ and the ratio θ/θ_t is more readily computed for all of these cases by means of the following expression:

$$\theta/\theta_t = \frac{C_F^{a-1}\,(k\theta)_{\text{Eqs. 10 and 11}}}{C_F^{a-1}\,(k\theta_t)_{\text{Eq. 8}}} = \frac{(a-1)x}{(1-x)^a[(1-x)^{1-a}-1]} \quad \ldots\ldots(51)$$

Some expressions are also indeterminate at $m = 0$. It can be seen readily that the ratio θ/θ_t is always equal to unity in this case because the reactor considered is a tubular one.

b) Model MT

1. *Conversions obtained for a given residence time.*

This model shows conditions similar to those of model TM except that here the reactants enter a zone of perfect mixing of volume mV and then travel in piston flow through a section of volume $(1 - m)\ V$. This is the equivalent of a CSTR of volume mV followed by a tubular reactor of volume $(1 - m)\ V$ as in Figure (11b). Such a combination has been discussed by Zwietering [38] and also by Trambouze and Piret [39], in a recent study dealing with the combination of reactors giving optimum conversion.

Referring to Figure (11) and applying Equation (10) the feed and intermediate concentrations of the reactors are related as follows:

$$C_F - C_i = \frac{r'm\ V}{q} \quad \ldots\ldots(52)$$

For the tubular zone, Equation (1) gives:

$$-\int_{C_i}^{C_E} \frac{dC}{r_t} = \frac{(1-m)\ V}{q} \quad \ldots\ldots(53)$$

The performance of a model MT reactor is obtained by a comparison similar to that developed for model TM. If the reactor was tubular the inlet and effluent concentrations would be related to the residence times θ_t, or V/q, by means of Equation (8). The latter, combined with Equation (52), for reaction orders other than unity, gives:

$$C_F = C_t + \frac{m}{a-1}\,C_i^a\,(C_t^{1-a} - C_F^{1-a}) \quad \ldots\ldots(54)$$

Combining Equations (8) and (53), one obtains:

$$C_i^{1-a} = C_E^{1-a} - (1-m)\,(C_t^{1-a} - C_F^{1-a}) \quad \ldots\ldots(55)$$

which, when introduced in Equation (54), gives the desired relations.

For zero-order reactions, as should be expected, Equations (54) and (55) give the same results as those obtained with model TM since $x = x_t$ irrespective of the degree of mixing.

For a second-order reaction, involving only one reactant, combination of Equations (54) and (55) gives:

$$m = \frac{(C_F/C_t - C_F/C_E) + \sqrt{C_F/C_t - C_F/C_E}}{C_F/C_t - 1} \quad \ldots\ldots(56)$$

or, in terms of conversion:

$$m = \frac{x_t - x}{x_t(1-x)} + \sqrt{\left(\frac{x_t - x}{x_t(1-x)}\right)\left(\frac{1-x_t}{x_t}\right)} \quad \ldots\ldots(57)$$

The variation of x as a function of m is shown for this case in Figure (14), at values of V/q corresponding to various conversions, x_t.

When two reactants are present, the following expression is obtained:

$$\frac{R}{R-1}\left[1 - \frac{1-x}{R-x}\left(\frac{R-x_t}{R(1-x_t)}\right)^{1-m}\right]^2 = 1 + \frac{1-x}{R-x}\left[ln\left(\frac{R-x_t}{R(1-x_t)}\right)^m - 1\right]\left[\frac{R-x_t}{R(1-x_t)}\right]^{1-m} \quad \ldots\ldots(58)$$

When $R = 1$, the case reverts to one of a second-order reaction and Equation (57) applies.

For other orders of reaction, the combination of Equations (54) and (55) gives the following expressions:

---

for $a = 0.5$

$$m = \frac{\sqrt{[(C_F/C_t)^{0.5} - 1]\left[(C_F/C_t)^{0.5} - 1 + 2\left(\frac{C_F/C_t}{C_F/C_E}\right)^{0.5}\right]} - \left(\frac{C_F/C_E - 1}{C_F/C_E}\right)C_F/C_t}{(C_F/C_t)^{0.5} - 1} \quad \ldots\ldots(59)$$

for $a = 1.5$:

$$m^3 - 3\left[\frac{(C_F/C_t)^{0.5} - 1 - (C_F/C_E)^{0.5}}{(C_F/C_t)^{0.5} - 1}\right]m^2 + 3\left[\frac{(C_F/C_E - 1) - [(C_F/C_t)^{0.5} - 1][2(C_F/C_E)^{0.5} - (C_F/C_t)^{0.5} + 1]}{[(C_F/C_t)^{0.5} - 1]^2}\right]m -$$

$$\left[\frac{[3C_F/C_E - 1][(C_F/C_t)^{0.5} - 1] + [(C_F/C_t)^{0.5} - 1 - 3(C_F/C_E)^{0.5}][(C_F/C_t)^{0.5} - 1]^2 - (C_F/C_E)^{0.5}(C_F/C_E - 1)}{[(C_F/C_t)^{0.5} - 1]^3}\right] = O \quad \ldots\ldots(60)$$

for $a = 3$:

$$m^3 - 3\left[\frac{(C_F/C_t)^2 - (C_F/C_E)^2 - 0.25}{(C_F/C_t)^2 - 1}\right]m^2 + 3\left[\frac{[(C_F/C_t)^2 - 1][(C_F/C_t)^2 - 2(C_FC_t/_E)^2] + (C_F/C_E)^2[(C_F/C_E)^2 - 1]}{[(C_F/C_t)^2 - 1]^2}\right]m -$$

$$\left[\frac{[(C_F/C_t)^2 - 1]\{(C_F/C_E)^2[3(C_F/C_E)^2 - 2] - [(C_F/C_t)^2 - 1][3(C_F/C_E)^2 - (C_F/C_t)^2]\} - (C_F/C_E)^4[(C_F/C_E)^2 - 1]}{[(C_F/C_t)^2 - 1]^3}\right] = O \quad \ldots\ldots(61)$$

Values of m in Equations (60) and (61) are obtained by approximation.

Curves showing the variation of x with m for these cases are presented in Figure (19) for a residence time such that x_t would be 90%. The same remarks apply in this case as for those of Figure (15) pertaining to Model TM.

For the particular case of first-order reactions, the application of general Equations (52), (53) and (1) to Model MT leads to the same expressions, Equations (23) and (24), as were obtained for Model TM. The curves of Figure (13) can then be used in this case.

Indeed, for first-order reactions, it can be demonstrated that the results will always be the same for a given reactor, no matter where the zone of perfect mixing is located, as long as the residence time for all elements going through that zone is the same, and equal to $m\theta$, as in Figures 20(a) and (b). It would not apply in a reactor such as shown in Figures 20(c) and (d) because the residence time for elements going through the zone of perfect mixing in this case is θ.

2. *Residence times or volumes required for a given conversion.*

For the CSTR section of the reactor, referring to Figure 11, the following equation applies:

$$\frac{C_F - C_i}{C_i} = mk\theta \qquad (62)$$

In the tubular section that follows, one obtains:

$$-\int_{C_i}^{C_E} \frac{dC}{C^a} = (1 - m)\, k\theta \qquad (63)$$

For each reaction order, values of $k\theta$ are found for different m's at a given conversion, by combining Equations (62) and (63). They are then divided by the value of $k\theta_t$ obtained from Equation (1) for the corresponding value of x. The ratio θ/θ_t is thus obtained, as a function of m, for given values of the conversion.

Here again, a zero-order reaction gives $\theta/\theta_t = 1$ for all values of m.

In a first-order reaction, since Model MT behaves like Model TM, Equations (44) to (50) inclusive are applicable, as is Figure 18.

For a second-order reaction, when $m \neq 1$, the procedure described above leads to the ratio:

$$\frac{\theta}{\theta_t} = \frac{(2m - 1)(1 - x) + 2(1 - m) - \sqrt{[(2m - 1)(1 - x) + 2(1 - m)]^2 - 4(1 - m)^2 x}}{2(1 - m)^2 x} \qquad (64)$$

Curves derived from this expression are presented in Figure 21. It is interesting to note that for the limiting case of complete conversion, when $x = 1$, the ratio θ/θ_t given by Equation (64) reduces to the expression

$$(\theta/\theta_t)_{x=1} = \frac{1}{1 - m}$$

which happens to be the same as that of Equation (50) for first-order reactions.

When two reactants are present and $C_A \neq C_B$, the following is obtained:

$$\frac{R - 1}{R}\left[1 + \frac{1 - x}{R - x}\left(m(R-1)(C_{A_F} k\theta) - 1\right) e^{(R-1)(1-m)(C_{A_F} k\theta)}\right] = \left[1 - \frac{1 - x}{R - x}\, e^{(R-1)(1-m)(C_{A_F} k\theta)}\right]^2 \qquad (65)$$

The ratio θ/θ_t in this case would thus be:

$$\frac{\theta}{\theta_t} = \frac{(C_{A_F} k\theta)_{\text{Eq. 65}}}{\frac{1}{R - 1} ln \frac{R - x}{R(1 - x)}} \qquad (66)$$

Again, when R = 1, the case reverts to one of a second-order reaction and Equation (64) applies.

For a reaction order of 0.5, when $m \neq 1$, the ratio θ/θ_t is found to be:

$$\frac{\theta}{\theta_t} = \frac{\sqrt{1 - m^2 x} - \sqrt{1 - x}}{(1 - m^2)(1 - \sqrt{1 - x})} \qquad (67)$$

When $a = 1.5$, the ratio θ/θ_t involves approximation calculations. The value of $k\theta$ is first obtained from the expression:

$$(k\theta)^3 - \frac{6(k\theta)^2}{(1 - m)C_E^{0.5}} + 4\left[\frac{3(1 - m)\, C_F/C_E + 3m - 1}{(1 - m)^3 C_F}\right](k\theta) - 8\,\frac{C_F/C_E - 1}{C_F C_E^{0.5}(1 - m)^3} = O \qquad (68)$$

The value of $k\theta_t$ is then calculated for the same conversion, using Equation (1), and the ratio θ/θ_t is easily obtained in this manner.

A similar procedure is involved for $a = 3$. In this case, the value of $k\theta$, for $m \neq 1$, is found from:

$$(k\theta)^3 + \left[\frac{(3m - 2)^2 - 12(1 - m)^2(C_F/C_E)^2}{8(1 - m)^3 C_F^2}\right](k\theta)^2 + \left[\frac{(3m - 2) + 3(1 - m)(C_F/C_E)^2}{4(1 - m)^3 C_F^2 C_E^2}\right] k\theta - \frac{(C_F/C_E)^2 - 1}{8(1 - m)^3 C_F^2 C_E^4} = O \qquad (69)$$

For a conversion of 90%, Figure 22 shows the variation of θ/θ_t with m, for the different orders of reaction discussed above. Unlike the performance of model TM, it is seen that in model MT the relative residence times vary more and more rapidly with the degree of mixing as the order of reaction increases.

c) Comparison of Models TM and MT

For purposes of comparison, conversions have been calculated for Models TM and MT at a residence time such that x_t = 90%. The results, for different orders of reaction, are presented in Figures 23, 24, 25 and 26 and correspond to the solid curves. It may happen that at a given level of mixing, corresponding to a certain value of m, the well-mixed section in the reactor is located between two zones of tubular flow, as shown in Figures 20(a) and (b). Depending on the location of this zone, the resulting conversion will be in the shaded area on a horizontal line connecting the TM and MT curves. This is valid provided the combined residence time is between $(1 - m)\ \theta$ for all elements going through the tubular section.

Inspection of the preceding figures reveals that residence time studies, such as suggested by Sherwood [7], are not sufficient to predict the conversion in a given reactor. It is necessary indeed to know also the history of the various elements as they flow through the reactor since, at a given residence time, different conversions can be obtained depending on the pattern of mixing.

It is interesting to examine further the curves of Figures 23, 24, 25 and 26 at given values of m. For reaction orders

superior to unity, Model TM gives a higher conversion than Model MT, while the reverse is true for values of α inferior to unity. In the case of first-order reactions, equal conversions are obtained for both models.

A different basis of comparison consists in calculating the ratios θ/θ_t for a given conversion at different values of m. Various orders of reaction are considered and the results presented in Figures 27, 28, 29 and 30 for a 90% conversion.

The curves for the TM and MT models represent again limiting cases. Points lying in the shaded areas correspond to models in which the zone of perfect mixing is located as in Figures 20(a) and (b).

An inspection of the figures shows that for orders of reaction superior to unity, Model TM requires a shorter residence time than Model MT, to reach the same conversion. The reverse applies for reaction orders inferior to unity. No difference exists when $\alpha = 1$.

For the particular case of $m = 1$, values of θ/θ_t have been reported previously [2, 11, 12, 26, 36, 37] for different orders of reaction, but MacMullin and Weber[26] used the ratio θ_t/θ.

For second-order reactions in which $C_A \neq C_B$, curves showing the variation of θ/θ_t with the conversion have been presented by Groggins[37] and Corrigan and Young[12], when $m = 1$.

d) Graphical Methods

While design problems involving consecutive reactors can often be solved analytically, long and tedious calculations may be involved, as in the case of Models TM and MT. In order to facilitate the solution of such problems, graphical methods have been developed which involve, in part, a means of computation whereby the overall conversion for a number of reactors in series is obtained from the individual conversions.

Referring to Figure 31(a), one can imagine a particular reactor as being made up of b reacting zones in series, each zone acting either as a tubular or a CST reactor. It could also be considered as consisting of b different reactors in series, as in Figure 31(b).

Since the effluent of one zone or reactor becomes the feed of the next, stepwise calculations are involved.

Let $x_1, x_2, \ldots x_i \ldots x_{b-1}, x_b$, be the individual conversions for each of the b zones. Then, introducing Equation (4) one obtains:

$$1 - x_1 = \frac{C_1}{C_F}$$

$$1 - x_2 = \frac{C_2}{C_1}$$

$$\vdots$$

$$1 - x_i = \frac{C_i}{C_{i-1}}$$

$$\vdots$$

$$1 - x_{b-1} = \frac{C_{b-1}}{C_{b-2}}$$

$$1 - x_b = \frac{C_b}{C_{b-1}}$$

Since $C_b = C_E$, combining the above expressions gives:

$$(1 - x_1)(1 - x_2)\ldots(1 - x_i)\ldots(1 - x_{b-1})(1 - x_b) = \frac{C_E}{C_F} \quad \ldots(70)$$

But the overall conversion x for the system, as defined already, is :

$$1 - x = C_E/C_F$$

By comparison with Equation (70), the overall conversion is thus related to the individual conversions by the expression:

$$1 - x = (1 - x_1)(1 - x_2)\ldots\ldots\ldots\ldots(1 - x_b)\ldots(71)$$

It may be noted that this expression is general because the particular conversion for any given zone or reactor involves only the feed and effluent concentrations, irrespective of the order of reaction, the size of the reacting zone or even the degree of mixing.

It is interesting to apply Equation (71) in the particular case of first-order reactions, for a system consisting of b identical CST reactors in series, the residence time for each being θ''. The overall conversion for the system is given by:

$$x = 1 - \frac{1}{(1 + k\theta'')^b} \quad \ldots\ldots\ldots\ldots\ldots\ldots(72)$$

which is equivalent to the expressions derived by MacMullin and Weber[26] and by Eldridge and Piret[27]. If the residence time was θ for the whole system, the residence time in each reactor would be θ/b and Equation (72) would become:

$$x = 1 - \frac{1}{\left(1 + \frac{k\theta}{b}\right)^b} \quad \ldots\ldots\ldots\ldots\ldots\ldots(73)$$

As the value of b in this expression increases, the value of x becomes equal to that of x_t in Equation (74) for a tubular reactor, indicating that, as expected, an infinite number of CSTR in series gives the same result as a tubular reactor of the same total residence time.

In the application of Equation (71), the conversion in each reacting zone or reactor is determined graphically. This process is facilitated by means of Figures 32, 33 and 34, each of which presents together the curves for tubular and CST reactors. Similar curves, for one or more orders of reaction, have been presented by various authors[16, 26, 27].

For first-order reactions, Figure 32 shows the variation of x_t or x_M as a function of $k\theta$. It is a plot of Equations (74) and (75) obtained by re-arranging Equations (5) and (12) respectively:

$$x_t = 1 - e^{-k\theta} \quad \ldots\ldots\ldots\ldots\ldots\ldots(74)$$

$$x_M = \frac{k\theta}{1 + k\theta} \quad \ldots\ldots\ldots\ldots\ldots\ldots(75)$$

Figure 33, for second-order reactions, is a plot of Equations (6) and (13), while Figure 34, for third-order reactions, corresponds to Equations (7) and (14).

If general Equation (71) is now applied to Models TM or MT, it becomes:

$$1 - x = (1 - x_t')(1 - x_m') \quad \ldots\ldots\ldots\ldots\ldots\ldots(76)$$

in which x_t' and x_M' represent the conversions in the tubular and CST portions of the reactor respectively.

This equation is used together with the following expression, which is equivalent to that relating partial residence times to the overall for the reactor:

$$C_F^{a-1}(k\theta) = C_F^{a-1}(k\theta)_M' + C_F^{a-1}(k\theta)_t' \quad \ldots\ldots\ldots\ldots\ldots\ldots(77)$$

where θ_M' is the residence time for the CSTR section and equal to $m\theta$. This is preferred to the form $\theta = \theta_M' + \theta_t'$, for convenience.

Together, they make for an easy solution of the different problems pertaining to TM and MT reactors in which it is required to determine one of the three quantities m, θ, x, when two are known. Although details of application vary slightly according to the order of reaction, especially for first-order reactions in which the term C_F^{a-1} in Equation (77) drops out, the method will be outlined in a general way. Specific examples are worked out in the Appendix.

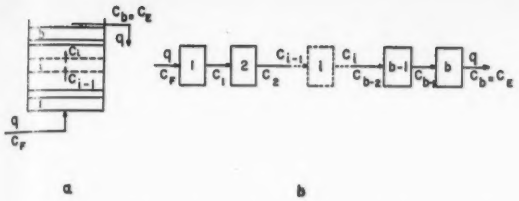

Figure 31—(a) reactor with b reacting zones in series. (b) system comprising b different reactors in series.

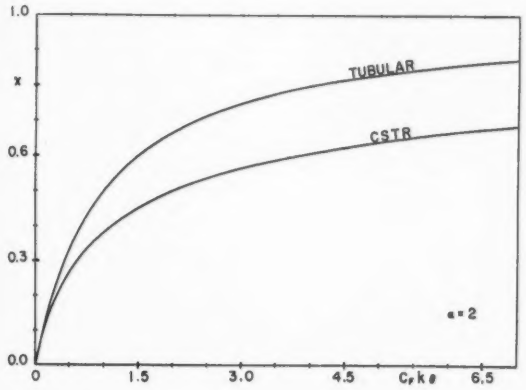

Figure 33—Variation of the conversion x with $C_F k\theta$, in CSTR and tubular reactors, for second-order reactions.

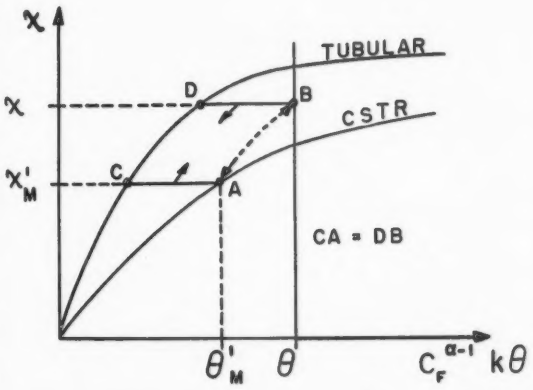

Figure 35—Graphical construction for determining m or the conversion in MT reactors.

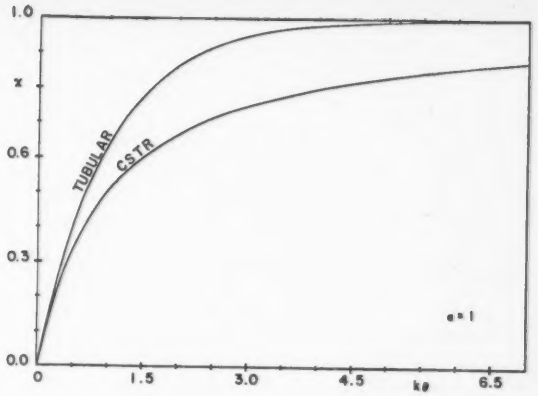

Figure 32—Variation of the conversion x with $k\theta$, in CSTR and tubular reactors, for first-order reactions.

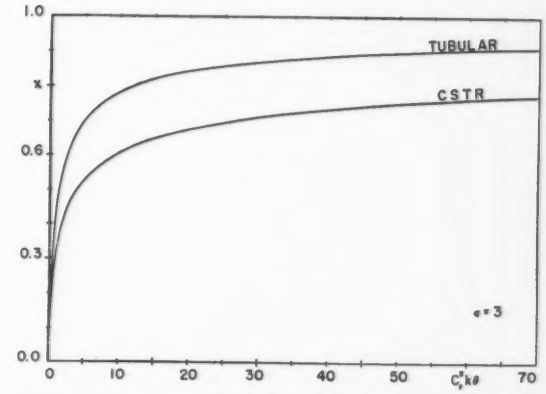

Figure 34—Variation of the conversion x with $C_F^2 k\theta$, in CSTR and tubular reactors, for third-order reactions.

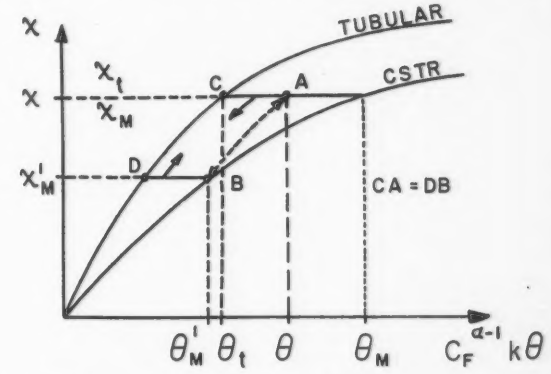

Figure 36— Graphical construction for determining relative residence times or m in MT reactors.

1. *Determination of the overall conversion x when m and θ are known.*

As in the analytical method it is necessary to distinguish between models TM and MT.

Model TM:

The first step consists in determining x_t'. Since m is known, it follows that:

$$C_F^{a-1}(k\theta)_t' = (1 - m)C_F^{a-1}(k\theta) \quad \ldots\ldots\ldots\ldots (78)$$

and

$$C_F^{a-1}(k\theta)_M' = m\, C_F^{a-1}(k\theta) \quad \ldots\ldots\ldots\ldots\ldots (79)$$

Depending on the order of reaction, x_t' is read from the curve for tubular reactors, in Figures 32, 33 or 34. It is to be noted that the abscissa in these Figures contains the term C_F^{a-1}. This refers to the particular feed concentration of the reacting zone or reactor considered.

In this particular case, after a conversion of x_t' in the first part of the reactor, the feed of the CST section will be:

$$C_F' = C_F(1 - x_t')$$

and thus the conversion x_M' will be read at an abscissa of $(C_F')^{a-1}(k\theta)_M'$ on the appropriate Figure. The values of x_t' and x_M' are then introduced into Equation (76) to give the overall conversion x.

Model MT:

In this case, x_M' is read on the CSTR curve of the appropriate Figure, at an abscissa of $C_F^{a-1}(k\theta)_M'$, or, $m\, C_F^{a-1}(k\theta)$.

The concentration of the feed to the tubular section is given by:

$$C_F' = C_F(1 - x_M')$$

The conversion x_t' is then read at an abscissa of $(C_F')^{a-1}(k\theta)_t'$, and the overall conversion computed by means of Equation (76).

Alternate Method:

A more simple method yet is available for the special case of MT reactors. It consists in a graphical construction applicable to either one of Figures 32, 33 or 34.

In a general way, one proceeds as in Figure 35, which can represent any one of these three Figures. The conversion x_M' is located on the CSTR curve at an abscissa of $C_F^{a-1}(k\theta)_M'$, determining point A. A path AB is then followed, parallel to the portion CD of the curve for tubular reactors, such that the abscissa of point B be $C_F^{a-1}(k\theta)$. The conversion indicated by point B is the overall conversion for the reactor.

A similar graphical construction does not apply to Model TM. It applies to Model MT because it can be shown that segment DB is equal to segment CA. Indeed, the two sides of the expression

$$C_F^{a-1}(k\theta) - C_F^{a-1}(k\theta)_t \text{ at } x = C_F^{a-1}(k\theta)_M \text{ at } x_M' - C_F^{a-1}(k\theta)_t \text{ at } x_M' \quad \ldots\ldots(80)$$

represent segments DB and CA respectively. When verified mathematically, Equation (80) works out to be an identity for all values of $C_F^{a-1}(k\theta)_M$ lying between 0 and $C_F^{a-1}(k\theta)$. In other words, it is valid for all values of m between 0 and 1.

2. Determination of relative residence time, θ/θ_t, when x and m are known.

Model TM:

A trial and error method is involved which nevertheless yields results rapidly. Once a value of θ is assumed, θ_t' is introduced in the term $C_F^{a-1}(k\theta)_t'$ to give a corresponding value of x_t', using the appropriate Figure 32, 33 or 34. Equation (76) is then used to compute the value of x_M' which in turn serves to determine graphically the value of $(C_F')^{a-1}(k\theta)_M'$. When divided by $(1 - x_t')^{a-1}$, the latter gives the value of $C_F^{a-1}(k\theta)_M'$.

If the sum of θ_t' and θ_M' thus obtained does not verify the value assumed originally for θ, the procedure is repeated until it does.

Since θ_t can be read directly on the curve for tubular reactors, using the appropriate Figure, at the conversion considered, the ratio θ/θ_t is readily obtained.

Model MT:

A procedure similar to the above is followed except that a value of θ_M' is first used, and x_t' is then computed to give $(C_F')^{a-1}(k\theta)_t'$. Dividing this value by $(1 - x_M')^{a-1}$ yields $C_F^{a-1}(k\theta)_t'$.

As in the preceding case, the procedure is repeated until the sum of θ_M' and θ_t' is equal to the value assumed for θ.

Alternate Method:

A graphical construction is again available for the particular case of MT reactors.

Figure 36 represents curves for tubular and CST reactors, for any order of reaction, as in Figures 32, 33 or 34.

A value of θ is assumed and the resulting abscissa $C_F^{-1}(k\theta)$ determines point A for the given conversion x. Following path AB parallel to CD determines at B the value of the abscissa $C_F^{a-1}(k\theta)_M'$. Dividing the latter by $C_F^{a-1}(k\theta)$ gives a value of m which, if unequal to the original one, requires that a new value of θ be chosen and the procedure repeated until the value of m obtained agrees with the given one.

It can be shown that the two sides of an expression similar to Equation (80), corresponding to segments AC and BD, are identically equal for all values of m between 0 and 1.

3. Determination of m when θ and x are known.

Model TM:

A trial and error procedure is indicated. Assuming a value of m, the corresponding conversion is calculated according to the method outlined already for determining the overall conversion when m and θ are known. Should the result differ from the value given, the procedure is repeated until agreement is reached.

Model MT:

Although one can proceed as with model TM, an alternate graphical construction is more suitable.

Referring to Figure 36, the values of θ and x determine point A. Following path AB parallel to CD, point B determines the value of θ_M' from which m is obtained directly since $m = \theta_M'/\theta$.

B. Partial Mixing and Short-Circuiting

The concept of short-circuiting has been used differently by various authors [3, 7, 8, 15, 26, 33] as either mathematical and statistical by -passing or channelling in a system. Short-circuiting in a reacting system refers, in the present work, to a portion of the feed which passes directly to the outlet without having reacted or been retained [22, 40].

Referring to Figure 12, the general equation for partial mixing and short-circuiting has been presented by Cholette and Cloutier [22], as their Equation (8), which reads:

$$m = \left(\frac{C_F - C_E}{C_F - C_M}\right) \cdot \frac{r_M}{r'} \quad \ldots\ldots(81)$$

The expressions for the reaction rates r_M and r' are:

$$r_M = k\, C_M^a \quad \ldots\ldots(11)$$

$$r' = k\, C'^a \quad \ldots\ldots(82)$$

The concentration C' in the zone of perfect mixing, derived from a material balance, is given by the following expression:

$$C' = \frac{C_E - (1 - n)C_F}{n} \quad \ldots\ldots(83)$$

Introducing Equations (11), (82) and (83) into Equation (81) the general expression reduces to the following in the case of one reactant:

$$m = \left(\frac{C_F/C_E}{C_F/C_M}\right)^{a-1} \left(\frac{C_F/C_E - 1}{C_F/C_M - 1}\right) \left(\frac{n}{1 - (1 - n)C_F/C_E}\right)^a \quad \ldots\ldots(84)$$

or, in terms of conversion, to

$$m = \frac{x}{x_M} \left(\frac{n(1 - x_M)}{n - x}\right)^a \quad \ldots\ldots(85)$$

It may be observed in Equation (84) that the last term drops out when short-circuiting is absent, whatever the order of reaction. Furthermore, in Equation (85), $x = x_M$ when n and m are equal to unity.

A further observation shows that the term $(n - x)$ in Equation (85) is always positive as x is always smaller than n, or equal to it for the limiting case of complete conversion.

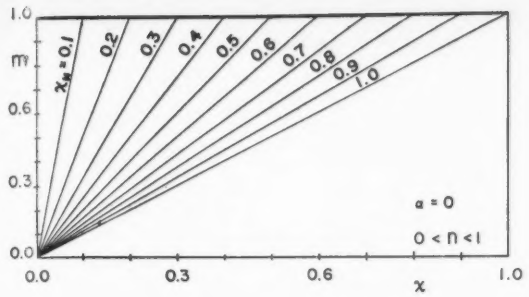

Figure 37—Variation of the conversion with m, in reactors with partial mixing and short-circuit, for zero-order reactions, at residence times such that the conversion in a CSTR is x_M, as indicated on curves.

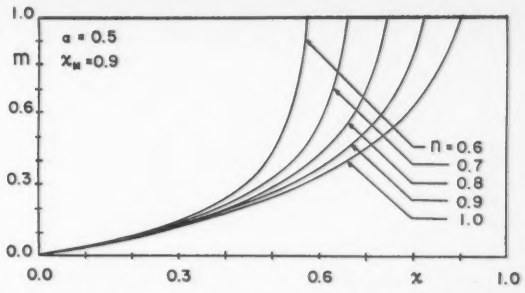

Figure 38—Variation of the conversion with m and effect of the short-circuit, in reactors with partial mixing and short-circuit, for α = 0.5, at a residence time such that the conversion in a CSTR would be 90%.

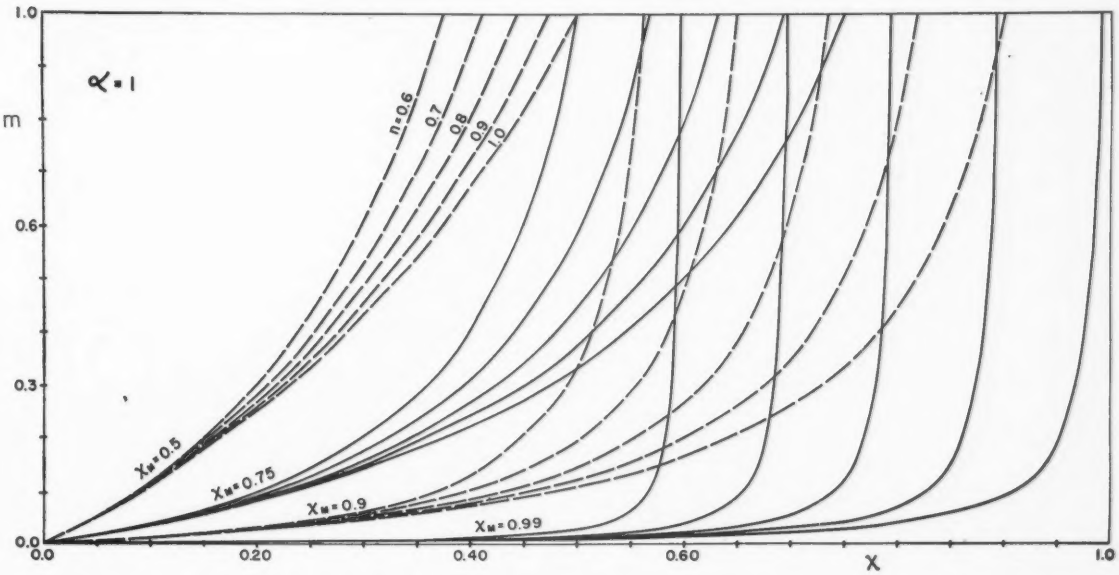

Figure 39—Variation of x with m, in reactors with partial mixing and short-circuit, for first-order reactions, at residence times such that the conversion x_M in a CSTR would be as indicated for each family of curves. The effect of the short-circuit, within a family of curves, is characterized by the values of n.

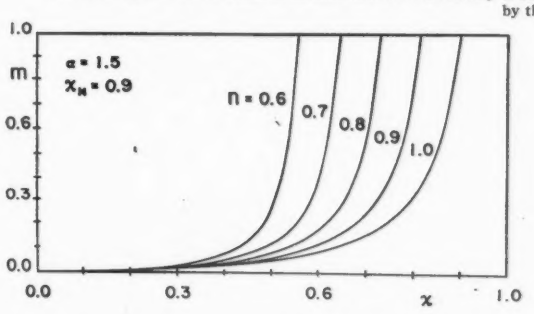

Figure 40—Variation of the conversion with m and effect of the short-circuit, in reactors with partial mixing and short-circuit, for α = 1.5, at a residence time such that x_M = 90%.

In the latter case, $C' = 0$ and from Equation (83), $C_E = (1 - n)C_F$. Now, applying the definition of conversion, as given by Equation (4), one obtains for the limiting case:

$$x = \frac{C_F - (1 - n)C_F}{C_F} = n$$

While Equations (84) and (85) are the general solutions for the model of Figure 12, many particular solutions have been worked out, depending on the order of reaction and on the magnitude of the short-circuit. For purposes of comparison, the results are presented under two headings.

a) ***Variation of the conversion with m, for a given order of reaction, at different values of the short-circuit.***

General Equation (85), applied to different orders of reaction, gives the following results:

1) $\alpha = 0$

For such reactions, the short-circuit effect cancels out[22]:

$$m = \frac{x}{x_M} \qquad (86)$$

The conversion is thus dependent on the effective volume of mixing only. A plot of Equation (86), in Figure 37, gives straight lines of slopes $1/x_M$, at all values of n.

2) $\alpha = 0.5$

$$m = \frac{x}{x_M}\sqrt{\frac{n(1 - x_M)}{n - x}} \qquad (87)$$

The curves of Figure 38 show that as the short-circuit increases and the effective volume of mixing decreases, the conversion x departs more and more from the theoretical value, x_M.

3) $\alpha = 1$

$$m = \frac{x}{x_M} \cdot \frac{n(1 - x_M)}{n - x} \qquad (88)$$

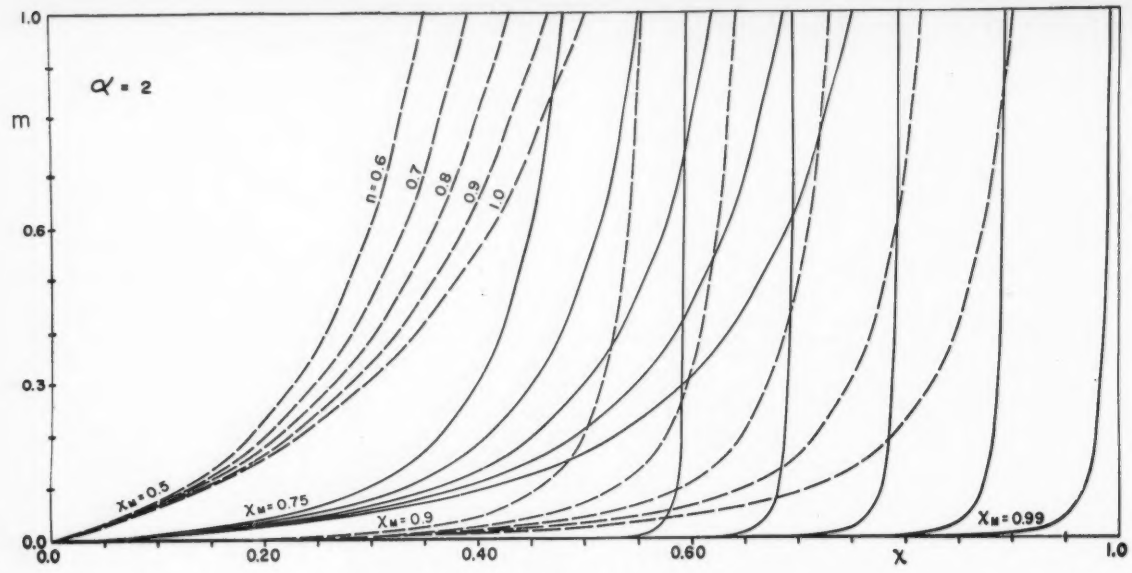

Figure 41—Variation of x with m, in reactors with partial mixing and short-circuit, for second-order reactions, at residence times such that the conversion x_M in a CSTR would be as indicated for each family of curves. The effect of the short-circuit, within a family of curves, is characterized by the values of n.

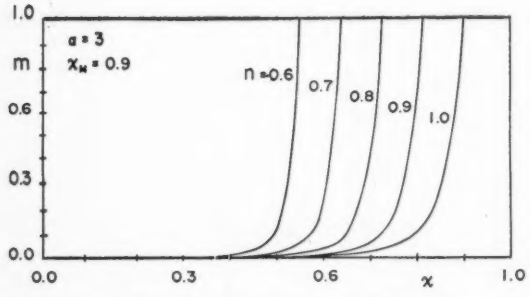

Figure 42—Variation of the conversion with m and effect of the short-circuit, in reactors with partial mixing and short-circuit, for $a = 3$, at a residence time such that $x_M = 90\%$.

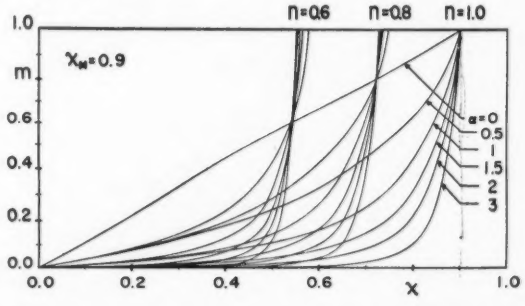

Figure 43—Variation of the conversion with m, in reactors with partial mixing and short-circuit, for different orders of reaction, at residence times such that $x_M = 0.9$. Each family of curves corresponds to a given value of the short-circuit.

Families of curves for first-order reactions are shown in Figure 39. They are plotted at different values of residence time θ_M corresponding to given theoretical conversions x_M. Values of $(1 - n)$ ranging up to 0.4 are presented to show the dominant effect of the short-circuit at higher conversions

4) $a = 1.5$

$$m = \frac{x}{x_M}\left(\frac{n(1 - x_M)}{n - x}\right)^{1.5} \quad \ldots\ldots\ldots\ldots\ldots\ldots (89)$$

a plot of which is shown in Figure 40.

5) $a = 2$

$$m = \frac{x}{x_M}\left(\frac{n(1 - x_M)}{n - x}\right)^{2} \quad \ldots\ldots\ldots\ldots\ldots\ldots (90)$$

Families of curves derived from Equation (90) are presented in Figure 41. As for first-order reactions, the effect of n becomes dominant as the theoretical conversion x_M increases. At lower values of x_M, the influence of m becomes more appreciable.

When two reactants undergo a second-order reaction and are present in unequivalent molar amount, the following will apply:

$$m = \frac{x}{x_M} \cdot \frac{n^2(1 - x_M)(R - x_M)}{(nR - x)(n - x)} \quad \ldots\ldots\ldots\ldots\ldots\ldots (91)$$

which reverts to Equation (90) when $R = 1$.

6) $a = 3$

$$m = \frac{x}{x_M}\left(\frac{n(1 - x_M)}{n - x}\right)^{3} \quad \ldots\ldots\ldots\ldots\ldots\ldots (92)$$

a plot of which is shown in Figure 42 for a theoretical conversion x_M of 0.9.

b) *Variation of the conversion with m, at a given short-circuit, for different orders of reactions.*

Figure 43 shows how the degree of completion of a reaction, or conversion, is affected by the three variables m, n and a, at a theoretical conversion x_M of 0.9.

The presence of a short-circuit is generally the determining factor affecting conversion, except at low values of m. At a certain value of n, for a given short-circuit, the mixing level has a more and more pronounced effect as the order of reaction decreases; as high values of m are reached, the conversion becomes approximately the same for all orders of reaction.

Generally, it is observed that for given values of m and n, the conversion increases with increasing orders of reaction at all values of m smaller than n. The reverse is true for values of m larger than n. When $m = n$, the conversion is the same for all orders of reaction, as indicated by the curves of one family crossing each other at a single point.

CONCLUSIONS

The present study should help to throw light on the performance of chemical reactors in general because, as pointed out by Smith [1], no correlations were available yet in the chemical engineering literature for partially mixed reactors. Although rather simple models have been investigated, there should follow a better understanding of the relative importance of different factors affecting the behavior of actual reactors.

As further investigations are carried out, other models [22] will be considered and in addition more factors may have to be taken into account such as actual mixing patterns, turbulence, diffusion and mass transfer from one zone to another.

While this study is restricted to homogeneous, irreversible and isothermal reactions, other interesting results are anticipated when reversible, consecutive, or simultaneous reactions are carried out isothermally or adiabatically, in models such as those defined in the present work.

It is evident that the scope of chemical kinetics is as yet unlimited and that a great number of promising research topics should be investigated in order to secure sound information on the phenomena intimately associated with chemical processes [41].

Although reactors must be designed and built even when data or rigorous design procedures are not available [42], the ever increasing contributions to the subject add to the scientific and mathematical background of reactor design.

Acknowledgement

The authors wish to express their appreciation to the National Research Council of Canada for grants-in-aid of this study and to Laval University for financial support.

Nomenclature

A = refers to reactant A
B = refers to reactant B
C = volumetric concentration, lbs./ft.^{3}
- C_E = effluent concentration.
- C_F = feed concentration to the reactor.
- C_F' = feed concentration to the second zone of a reactor, models TM or MT.
- C_i = intermediate concentration in a reactor, as the reactants leave one reacting zone and enter another.
- C_M = theoretical concentration of the effluent if mixing was perfect.
- C_t = theoretical concentration of the effluent if the reactor was tubular.
- C' = concentration in a zone of perfect mixing.

k = velocity rate constant (lbs./ft.^{3})$^{1-a}$/hr.
m = fraction of the total volume which is perfectly mixed.
n = fraction of the feed entering the zone of perfect mixing.
q = volumetric rate of flow, ft.^{3}/hr.
r = reaction rate, lbs./(ft.^{3})(hr.)
- r_M = reaction rate, for a CSTR.
- r_t = reaction rate, in the tubular zone of a TM or MT reactor.
- r' = reaction rate for the well-mixed zone of a reactor.

u = fraction of the total volume undergoing piston flow (special case: Figure 20).
V = volume, ft.^{3}
x = conversion or degree of completion of a reaction $= \dfrac{C_F - C_E}{C_F}$
- x_M = theoretical conversion in a CSTR.
- x_t = theoretical conversion in a tubular reactor.
- x_M' = conversion in the CST section of a TM or MT reactor.
- x_t' = conversion in the tubular section of a TM or MT reactor.

a = order of a reaction.
$\theta = V/q$ = residence time, hr.
- θ_M = residence time of a CSTR.
- θ_t = residence time of a tubular reactor.
- θ_M' = residence time of the CST section of a TM or MT model.
- θ_t' = residence time of the tubular section of a TM or MT model.
- θ'' = residence time of one reactor in a system of b identical CSTR's in series (Special case: Equation (72)).

References

(1) Smith, J. M., "Chemical Engineering Kinetics", McGraw-Hill Book Co., New York, 1956.
(2) Gilliland, E. R., and Mason, E. A., Ind. Eng. Chem., **44,** 218 (1952).
(3) Gilliland, E. R., Mason, E. A., and Olivier, R. C., Ind. Eng. Chem. **45,** 1177 (1953).
(4) Danckwerts, P. V., Chem. Eng. Sci., **2,** 1 (1953).
(5) Danckwerts, P. V., Jenkins, J. W., and Place, G., Chem. Eng. Sci., **3,** 26 (1954).
(6) Danckwerts, P. V., Ind. Chemist. **30,** 102 (1954).
(7) Sherwood, T. K., Chem. Eng. Prog., **51,** 303 (1955).
(8) Handlos, A. E., Kunstman, R. W., and Schissler, D. O., Ind. Eng. Chem., **49,** 25 (1957).
(9) Hull, D. M., and Kent, J. W., Ind. Eng. Chem., **44,** 2745 (1952).
(10) Singer, E., Todd, D. B., and Guinn, V. P., Ind. Eng. Chem., **49,** 11 (1957).
(11) Lessels, G. A., Chem. Eng., **64** (8), 251 (1957).
(12) Corrigan, T. E., and Young, E. F., "CE Refresher" Chem. Eng., Sept. 1955 through March 1956.
(13) Young, E. F., Chem. Eng., **64** (2), 241 (1957).
(14) Greenhalgh, R. E., Johnson, R. L., and Nott, H. D., Chem. Eng. Prog., **55,** 44 (1959).
(15) Weber, A. P., Chem. Eng. Prog., **49,** 26 (1953).
(16) Nagata, S., Eguchi, W., Inamura, T., Tanigawa, K., and Tanaka, T., Chem. Eng. (Japan), **17,** 387 (1953).
(17) Kramers, H., and Alberda, G., Chem. Eng. Sci., **2,** 173 (1953).
(18) Wehner, J. F., and Wilhem, R. H., Chem. Eng. Sci., **6,** 89 (1956).
(19) Bernard, R. A., and Wilhem, R. H., Chem. Eng. Prog., **46,** 233 (1950).
(20) Carberry, J. J., Can. J. Chem. Eng., **36,** 207 (1958).
(21) Carberry, J. J., and Bretton, R. H., A.I.Ch.E. Journal, **4,** (3), 367 (1958).
(22) Cholette, A., and Cloutier, L., Can. J. Chem. Eng., **37,** 105 (1959).
(23) Chu, J. C., Chem. Eng., 63 (11), 215 (1956); 63 (12), 183 (1956); 64 (1), 235 (1957).
(24) Hougen, O. A., and Watson, K. M., "Chemical Process Principles", Part III, John Wiley and Sons, Inc., New York, 1947.
(25) Daniels, F., Ind. Eng. Chem., **35,** 504 (1943).
(26) MacMullin, R. B., and Weber, M., Jr., Trans. Amer. Inst. Chem. Engrs., **31,** 409 (1935).
(27) Eldridge, J. W., and Piret, E. L., Chem. Eng. Prog., **46,** 260 (1950).
(28) Caddell, J. R., and Hurt, D. M., Chem. Eng. Prog., **47,** 333 (1951).
(29) Jenney, T. M., Chem. Eng., **62** (12), 198 (1955).
(30) Nord, M., Chemical Industries, **63,** 666 (1948); **64,** 280 (1949).
(31) Bosworth, R. C. L., Phil. Mag., **39,** 847 (1948); **40,** 314 (1949).
(32) Denbigh, K. G., J. Appl. Chem., **1,** 227 (1951).
(33) Denbigh, K. G., Trans. Faraday Soc., **40,** 352 (1944).
(34) Stead, B., Page, F. M., and Denbigh, K. G., Disc. Faraday Soc., p. 263 (1947).
(35) Leclerc, V. R., Chem. Eng. Sci., **2,** 213 (1953).
(36) Reman, G. H., Chem. Ind., No. 3, 46 (1955).
(37) Groggins, P. H., "Unit Processes in Organic Synthesis", 5th Ed. Chap. 3, McGraw-Hill Book Co., New York, 1958.
(38) Zwietering, Th. N., Chem. Eng. Sci., **11,** 1 (1959).
(39) Trambouze, P. J., and Piret, E. L., A.I.Ch.E. Journal, **5,** (3), 384 (1959).
(40) MacDonald, R. W., and Piret, E. L., Chem. Eng. Prog., **47,** 363 (1951).
(41) Hougen, O. A., "Reaction Kinetics in Chemical Engineering" Chem. Eng. Prog. Monograph Series No. 1, Vol. 47 (1951).
(42) Walas, S. M., Reaction Kinetics for Chemical Engineers, McGraw-Hill Book Co., New York, 1959.

APPENDIX

A few examples are worked out to illustrate as much as possible the various applications of the graphical methods described, changing not only the different parameters but also the form of solution.

(1) Find the conversion x, for Model TM or MT, given:

$$\alpha = 1,\ k\theta = 2.30,\ m = 0.3.$$

$$(k\theta)'_M = (0.3)\ (2.3) = 0.69$$

and from Figure 32, $x'_M = 0.41$

$$(k\theta)_t' = (0.7)\ (2.3) = 1.61$$

From Figure 32, $x_t' = 0.8$

From Equation (76):

$$(1 - x) = (1 - 0.41)\ (1 - 0.8)$$

$$\therefore x = 0.88$$

Since for $k\theta_t = 2.3$, Figure 32 gives: $x_t = 0.9$, the actual conversion of 0.88 found above can be checked in Figures 13, 15, 19 or 24, at a conversion $x_t = 0.9$.

(2) Find m, using a graphical construction, for Models MT or TM, given $k\theta = 2.3$, $x = 0.88$, $\alpha = 1$.

Point B, in the general construction of Figure 35, is found to have the following coordinates, when using the proper curves, in Figures 32: (2.3, 0.88).

Following path BA parallel to DC, the abscissa of point A is found to be : $(k\theta)'_M = 0.69$

The value of m is then : $0.69/2.3 = 0.3$

(3) Find x, for Model TM, given: $C_F(k\theta) = 9.0$, $m = 0.9$, $\alpha = 2$.

$$C_F(k\theta)_t' = 0.1 \times 9 = 0.9$$

from Figure 33, $x_t' = 0.47$

$$C_F(k\theta)_M' = (0.9)\ (9) = 8.1$$

The value of $(C_F')\ (k\theta)'_M$ is thus:

$$8.1\ (1 - 0.47) = 4.3$$

From Figure 33, $x'_M = 0.62$

Equation (76) gives:

$$1 - x = (1 - 0.47)\ (1 - 0.62)$$

$$\therefore x = 0.8$$

If the reactor was tubular, a value of $C_F k\theta_t$ of 9.0 would give $x_t = 0.9$; the above conversion, $x = 0.8$, can be checked on Figures 14, 15 or 24.

(4) Find θ/θ_t, for Model TM, given: $\alpha = 2$, $x = 0.5$, $m = 0.83$. Assume a value of $C_F(k\theta)_t' = 0.25$.

From Figure 33, $x_t' = 0.2$

$$C_F(k\theta)'_M = \frac{(0.25)\ (0.83)}{(1 - 0.83)} = 1.22$$

$$(C_F')\ (k\theta)'_M = 1.22\ (1 - 0.2) = 0.98$$

Figure 33 gives then: $x'_M = 0.375$

Applying Equation (76):

$$1 - x = (1 - 0.2)\ (1 - 0.375)$$

$$\therefore x = 0.5$$

which checks the given conversion. Had it been different, a new value of $C_F(k\theta)_t'$ would have to be assumed and the procedure repeated until the conversion obtained would correspond to the given one.

Now, the total value of $C_F(k\theta)$ is:

$$0.25 + 1.22 = 1.47$$

At $x_t = 0.5$, Figure 33 shows that $C_F k\theta_t = 1$.

The required ratio θ/θ_t is then $1.47/1 = 1.47$ which checks the value given on Figure 16.

(5) Find θ/θ_t, using a graphical construction, for Model MT, given:

$$\alpha = 3,\ x = 0.9,\ m = 0.59.$$

Assume $C_F^2(k\theta) = 99$

Using Figure 34 and applying the construction of Figure 36 the abscissa of point B is found to be: $C_F^2(k\theta)'_M = 58.4$ It determines the value of m as $58.4/99 = 0.59$, which corresponds to the value given originally. If it had been different, other values of $C_F^2(k\theta)$ would have been assumed, until the resulting value of m agreed with that given.

To obtain a conversion of 0.9 in a tubular reactor, Figure 34 shows that $C_F^2 k\theta_t = 49.5$

The ratio θ/θ_t is then: $99/49.5 = 2$ which value can be checked in Figures 22 and 30.

(6) Find m for a MT reactor, given: $\alpha = 3$, $x = 0.9$, $\theta/\theta_t = 2$.

At $x_t = 0.9$, Figure 34 gives: $C_F^2 k\theta_t = 49.5$

Thus, $C_F^2(k\theta) = (2)\ (49.5) = 99$.

Assume now a value of $C_F^2(k\theta)'_M = 58.4$

Figure 34 gives $x_M' = 0.76$ and Equation (76) yields:

$$x_t' = 1 - \frac{1 - 0.9}{1 - 0.76} = 0.58$$

At $x_t' = 0.58$, Figure 34 gives: $(C_F')^2(k\theta)_t' = 2.34$ so that,

$$C_F^2(k\theta)_t' = \frac{2.34}{(1 - 0.76)^2} = 40.6$$

The total value of $C_F^2(k\theta)$ is: $58.4 + 40.6 = 99$ and checks the value derived at first from the given ratio θ/θ_t of 2.

If not the same, another value of $C_F^2(k\theta)'_M$ would have to be assumed and the procedure repeated until agreement was reached.

The value of m is obtained from the ratio:

$$\frac{C_F^2(k\theta)'_M}{C_F^2(k\theta)} = \frac{58.4}{99} = 0.59$$

Figures 22 and 30 verify this result.

A graphical construction, as in example 2, would give the same result without involving trial and error calculations.

* * *

The Incorporation of Fission Products into Glass for Disposal[1]

A. R. BANCROFT[2]

There is need of an economical and safe method of disposing of radioactive waste produced by nuclear reactors. A method for the incorporation of fission products into glass is being studied at Chalk River. Glass containing up to 50 curies of fission products per kilogram has been made during the investigation of the process. This radioactive glass has been used in stability studies in the laboratory and in the field.

Nepheline syenite (a rock containing *Na, K* and *Al* silicates) fluxed with up to 30% by weight of lime, is used as the base for the glass. A nitric acid solution of the fission products is added to a pelletized mixture of the solids. When the mixture is heated nitric acid is evaporated near 110°C. The nitrates are decomposed in the temperature range 130-600°, and the mixture is melted to form a glass at a maximum temperature of 1350°. Two of the fission products, ruthenium and cesium, are volatilized to varying degrees from the mixture during heating and create a major contamination and containment problem.

The method of processing and results obtained are discussed. The volatilized elements have been removed from the off-gas stream by a method which permits their incorporation into glass. Scale-up of the process to treat fission product wastes from power reactors should present no great difficulty other than design of equipment for the remote processing of large quantities of radioactive material at high temperature.

THE fission products generated by nuclear reactors are a biological hazard because they are radioactive. This radioactivity is eliminated only by natural decay, which occurs in times ranging from seconds to many years for the different nuclides. Two of the longer-lived nuclides, strontium-90 and cesium-137 represent a hazard for hundreds of years.

Spent fuel from a nuclear reactor may be processed by chemical extraction methods to separate the uranium and plutonium from the fission products. The fission products are concentrated in a nitric acid solution and this solution is stored as waste in metal tanks. If this method of storage were continued for the whole of the hazardous lifetime of the fission products it would be necessary to transfer the solution periodically to new tanks because for long periods, the tanks cannot be guaranteed against leakage. The cost of this storage is high.

In the future, when many nuclear reactors are used to generate electric power, the rate of production of fission products will be very much higher than it is now. The cost of treating the radioactive wastes for disposal will not represent a large percentage of the over-all cost of the electric power, but it may be an appreciable percentage of the cost of reprocessing fuel and it must be kept as low as possible; hence the need for an economical and safe disposal method for fission products. A safe method may be defined as one that does not allow significant quantities of fission products to escape to man's environment for many hundreds of years.

There are many methods of disposal being considered by groups in different countries. Some of these are listed as follows:

As solution
- (1) in metal tanks
- (2) in deep underground strata
- (3) in underground salt formations

As solids
- (4) solution converted to calcined solid
- (5) fission products incorporated into fired clay
- (6) fission products incorporated into glass.

Work is being done at Chalk River to develop a method of incorporating fission products into glass. Some of the desirable features of glass as a medium for disposal are as follows:

1. A greater variety of burial locations are available than for methods (2) and (3).
2. There is less risk of widespread dispersal of radioactivity from a solid disposal than there is from a liquid disposal.
3. The rate of release of fission products by water attack is lower from glass than it is from the calcined alumina (method 4); there is not enough information available to make a comparison with fired clay. The rate of dissolution in water is an important factor when considering solids, because buried in the ground, they may be in contact with ground water. If they released fission products to water at an unsafe rate they would have to be stored in water-proof containers, such as metal cans or concrete vaults, and this extra protection would add to the cost of the disposal. It is expected that glass can be made of such quality that it can be buried without added protection.

[1]*Manuscript received August 26; accepted October 5, 1959.*
[2]*Chemical Engineering Branch, Chemistry and Metallurgy Division, Atomic Energy of Canada Limited, Chalk River, Ont.*

Several years ago it was decided that experimental equipment should be built to handle one gallon batches of fission product solution. The purpose of building this equipment was twofold:

1. To prepare pieces of glass containing sufficiently large quantities of radioactivity to allow reliable tests to be done in the laboratory and in the field on the dissolution of glass in water.
2. To obtain information on operating problems, such as dusting, volatilization, handling and control.

During 1956 and 1957 equipment development, construction and testing were carried out, and in May 1958 the first block of highly active glass was produced. Since that time more than 2000 curies of fission products have been incorporated into glass, most of which is being used in leaching tests.

Cost estimates were made for incorporating the fission products in concentrated power-reactor wastes into glass by the process described in this paper. Processing costs were in the order of $0.05 per gram of fission products or $2 per kilogram of glass. These costs represented less than 1% of the cost of the electric power produced, but the additional expenses of disposing of the glass were considered to increase the over-all disposal cost to 1-2% of the power cost.

DESCRIPTION OF EQUIPMENT

In Figure 1 a schematic flowsheet of the process is shown. The solid and liquid ingredients are mixed in the crucibles in which the glass is to be melted. The crucibles are transferred from the mixing station to the drying and denitrating furnace, in which they are heated to a maximum temperature of 900°C. After this heating the mixes are allowed to cool over night, and then are placed in the melting furnace for further heating, to 1350° for one hour. The glass which is formed is cooled in the furnace before removal for testing. The gases generated in both these furnaces are drawn through a gas-cleaning system where the volatilized radioactivity is collected on adsorbers, the nitric acid is recovered in a packed column, and the remaining gases are passed through a caustic scrubber and filter before being exhausted.

Before a description is given of the equipment used for this work it should be mentioned that, because these fission products are highly radioactive, they must be handled with extreme care. Adequate shielding (four inches of lead or two feet of concrete for this equipment) must be provided to protect personnel from excessive exposure to radiation. All equipment used in the cells must be reliable and simple to maintain, because repairs can often be made only by remote methods. All handling systems must be suited to the use of hand-operated manipulators and pneumatic, hydraulic and electrically operated mechanisms. Thus in developing a process for handling radioactive materials attention must be given each operation. The simplest means are usually the best.

Figure 2 shows some of the equipment in the operating cell. This photograph was taken some time before the system was completed and is not accurate in all respects. As a guide to size, the crucibles are 8 in. in diameter at the top and 11 inches high. To the left of the photograph is the mixing station, a box that contains the crucible while the solution and solids are added. The shroud is lowered to cover the crucible while the solution is being added, and reduces the spread of activity by splashing. Liquid is added through the pipe entering the front of the box and pours into the middle of the crucible. The pelletized solids are also fed to the middle of the crucible, through a 1 in. pipe which is not shown. The box is fitted with a door moved hydraulically to cover the opening, has a water spray in it for washing, and is ventilated separately from the rest of the cell.

Each furnace can accommodate two crucibles. The furnaces are home-made and are in sections for easier disposal; they are heated by eight silicon carbide heating elements. Electrical connections to the elements are made by wires through holes in the ceiling and by spring-loaded contacts under the furnaces. These connections are necessary to allow the remote replacement of elements. The doors are moved by electric hoists. Inside the 12 kw. drying furnace, at the left, is a stainless steel can, which serves to contain the nitric acid fumes and volatilized activity. A cover for the can is fitted to the inside of the furnace door and can be pressed against the can by a hydraulic piston. The melting furnace (30 kw.), at the right, contains no metal but in it are two shallow silicon carbide receptables which are large enough to contain the glass from a crucible if it cracks.

In the centre of the photograph is an elevator which travels through a hole in the ceiling and is used to bring crucibles into the cell. Figures 3 and 4 show the handling tongs used to move the crucibles about in the cell. Once the glass has been prepared it is moved by means of a dolly on a track into an adjacent cell. This cell has provision for storing glass, removing it from the crucibles, leaching it in flowing or static water, and removing it from the cell for disposal. Figure 5 shows a crucible being placed into a leaching tank. The tongs are moved through a ball-and-socket joint in the ceiling and have air-operated jaws.

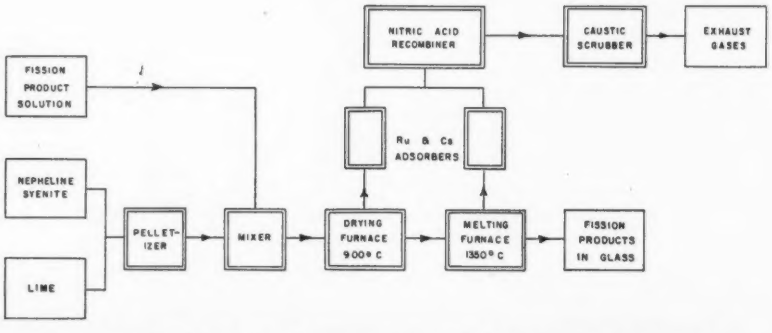

Figure 1—Flowsheet for the incorporation of fission products into glass.

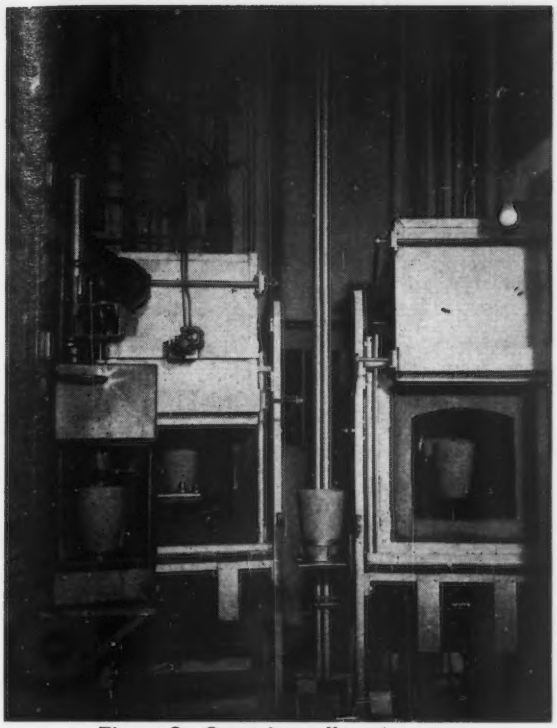

Figure 2—Operating cell equipment.

Figure 3—Handling a crucible inside cell with tongs.

Figure 4—Handling tongs outside 4-inch thick lead shielding wall, showing window and ball-and-socket joint for tongs.

Figure 5—Placing crucible into leaching tank.

DESCRIPTION OF PROCESS

Mixing

The composition of nepheline syenite (N.S.), a naturally occurring rock used in the glass, is given in Table 1.

TABLE 1
APPROXIMATE COMPOSITION OF NEPHELINE SYENITE

SiO_2	60%	Na_2O	10%
Al_2O_3	24%	K_2O	5%
	others 1%		

Nepheline syenite can be melted in the temperature range 1300-1400°C., but it is extremely viscous and cannot be made free of bubbles in a convenient heating time. However, if lime is added to the N.S. a bubble-free melt can be made by heating for times as short as one hour at 1350°. In experiments, up to 30% by weight of lime in N.S. is used, but the normal mix is 85% N.S.-15% *CaO*.

The waste solution which was used for the work described in this paper had the composition indicated in Table 2.

TABLE 2

ANALYSIS OF CONCENTRATED FISSION-PRODUCT SOLUTION
February, 1959

Acidity	8*N HNO*$_3$
Specific gravity	1.39
Total	8.6 x 10^9 β counts per minute per millilitre
Cs–137	4.0 x 10^9 " " " " " "
Ce–144 + *Pr*–144	8.6 x 10^8 " " " " " "
Sr–90 + *Y*–90	3.4 x 10^9 " " " " " "
Ru–106 + *Rh*–106	8.6 x 10^7 " " " " " "
Total solids	227 mg/ml (*Na, Fe, U, Ca, Al, Cr, Ni, Mg*)
Non-volatile solids	100 mg/ml

When the solution and solids are mixed together the nitric acid decomposes some of the N.S. and forms a silica gel. The gelling time for a mixture of this solution and pure N.S. is about 15 seconds. If 15% of lime is mixed with the N.S. before the solution is added the gelling time is somewhat longer, depending upon the method of mixing with the acid solution. Some heat is generated by the reaction and this can cause the temperature of the mixture to increase to the boiling point of HNO_3.

During the early development of the process using solutions which were not radioactive, a rotating stirrer was used to mix the solids and liquid. For some mixtures uniform blends were obtained by stirring for one minute and the stirrer could be removed before the mixture gelled. However, with some compositions the mixture gelled in a very short time and the stirrer was either trapped or had a large fraction of the mixture adhering to it on removal. A stirrer was therefore unsuitable for remote operation and the powdered nepheline syenite and lime are now mixed together and pelletized by rolling in a rotating drum. The pellets are screened and the −4 +20 mesh fraction is used. In this form the solids can be fed from a vibrating feeder, and mixed with the solution without stirring or agitation. The pellets have enough free space between them to allow the solution to soak through a layer several inches thick before gelling blocks the channels.

For convenience of operation the mixes are prepared by feeding a layer of pellets several inches deep into a crucible and then adding enough solution to react. Alternate additions of solids and liquid result in a layered mixture which has dry pellets as the top layer.

The silica gel formed in a mixture is generally quite firm, and after being dehydrated by heating it is very porous. This texture of the gel reduces the possibility of some of the mixture being "bumped" from the crucible during heating. In addition, the porous structure of the dried mixture provides channels through which gases leave the mix. These channels are tortuous and are probably efficient at de-entraining particles from the gases flowing in them. The entrainment losses from a mixture are less than 0.1%.

Drying and Denitrating

When a mixture of solution and solids is heated many reactions take place. At temperatures of 100-110°C. the water and nitric acid boil off. The silica gel is dehydrated in the range of 100-150°. At 135° aluminum nitrate decomposes to release oxides of nitrogen. At higher temperatures the nitrates of iron, sodium, potassium and calcium decompose, the latter at about 600°. Since the temperature of the mixture is not uniform during heating, it is probable that many of these reactions occur simultaneously. The maximum temperature of the first phase of the heating is 900°, which is high enough to ensure complete denitration, but does not cause rapid deterioration of the stainless steel can inside the furnace.

From the furnace the vapors and gases released during heating and the air entering through cracks are drawn through a gas-cleaning system. The volatilized radioactivity is collected on a granular adsorbent and the nitric acid and water are condensed in a column packed with Raschig rings. The oxides of nitrogen are scrubbed in the same column with a nitric acid solution to convert them to nitric acid. After passing through the condenser-recombiner the gases are bubbled through a solution of sodium hydroxide to remove entrained acid. They are then passed through a filter and exhausted to the building ventilation system.

Melting

The second phase of the heating is done in a furnace which can be heated to 1400°C. The gases from this furnace are also passed through the packed column, which, at this stage, is operated as a gas scrubber rather than a condenser–recombiner because most of the volume is air drawn in through cracks in the furnace.

After the mixes have been heated to 1350° and kept at that temperature for one hour, they are cooled slowly inside the furnace to anneal the glass. The temperature after 16 hours is about 300° and after another 24 is about room temperature. After this time the glass is removed for inspection and testing.

A photograph of a 2-kg. piece of 85% N.S.–15% *CaO* glass is shown as Figure 6. This glass is clear and almost colorless, but that made with fission product solution is dark brown, colored mainly by iron and chromium corrosion products. The upper surface is free from crust and foam, but there are a few surface bubbles evident. Parts of the curved surface were chipped away when the crucible was broken from the glass and some of the crucible clay was left adhering to the glass. The physical features of this specimen, except for color, are typical of the glass produced during this work.

Volatilization Losses

Two of the major fission products are volatile under conditions that exist during the heating of a mix. Ruthenium and cesium volatilize and escape to varying degrees from the mixes. This presents the most troublesome contamination problem of the process.

In a mixture containing free nitric acid most of the ruthenium which volatilizes escapes at temperatures

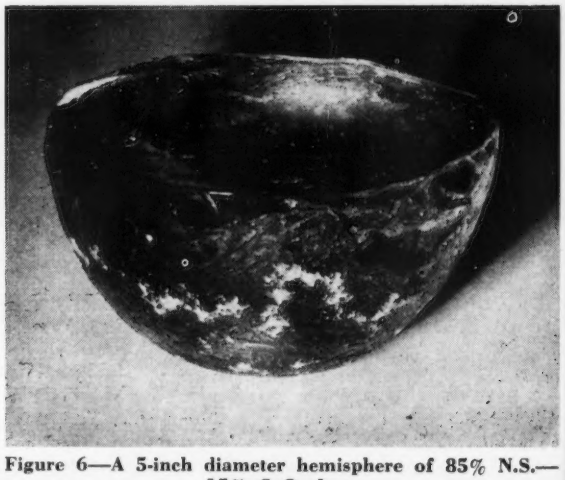

Figure 6—A 5-inch diameter hemisphere of 85% N.S.—15% *CaO* glass.

below 900°. If the acid is neutralized with lime then the losses occur mostly above 900°. The losses from both the acid and neutral mixes are about the same for a complete heating cycle. In the present equipment the volatilized activity can best be contained in the lower temperature range and the mixes are made to contain free nitric acid.

Experiments done at Chalk River by W. E. Erlebach indicate that most of the cesium that volatilizes leaves the mix in the temperature range 400-700°, but losses continue to occur to the maximum heating temperature of 1350°.

Ruthenium and Cesium Collection

Of course, it would be desirable to keep the ruthenium and cesium in the mix, but no suitable method of doing this has been found. Typical volatilization losses from a 2 kg. mix heated to 1350° are 50% of the ruthenium and 3% of the cesium. In the solution used, ruthenium represented about 1% of the total radioactivity, and the cesium was about 40%, so the loss from a mix was about 2% of the total activity. Two per cent of the total represents an appreciable amount of radioactive material and this could not be allowed to move uncontrolled through the equipment. It was therefore necessary to collect this volatilized activity in one location and in such form that it could be handled conveniently for disposal.

It was noticed in laboratory experiments that ruthenium was concentrated from the vapor on the stainless steel surfaces of the apparatus. It was believed that iron, or oxides of iron, had a great capacity for retaining ruthenium or its oxides. Experiments were done to test iron oxide as an adsorber of ruthenium. To provide a high surface area, porous firebrick that had been crushed to size −4 +20 mesh was soaked in a solution of ferric nitrate. The firebrick was dried and the nitrate decomposed by heating, leaving a coating of ferric oxide on the granules. Ruthenium volatilized from a mix, along with nitric acid vapor and air, was passed through a bed of the granular adsorbing material 4-in. deep. About 98% of the volatilized ruthenium remained on the adsorber. The same collecting efficiency was observed for adsorber temperatures up to 1000° and for superficial gas velocities up to one foot per second. This type of adsorber has been used successfully at the vapor outlets of the two furnaces.

Cesium was not adsorbed on iron as well as was ruthenium, but it did collect on any surface that was cool enough to allow it to condense. A bed of granulated firebrick coated with iron oxide could, therefore, be used to collect cesium if part of it were below 400°C.

In a future plant the adsorbing material used to collect most of the activity volatilized from mixes will contain only a small percentage of the through-put of fission-product activity. However, this amount of activity will be appreciable and should not be considered as a disposal separate from the glass. The present intention is to incorporate the adsorbing material into the glass. This addition will change the glass composition and may reduce the resistance to attack by water. This problem is under investigation.

LEACHING TESTS ON GLASS

One of the advantages of glass as a medium for disposing of fission products is its extremely low rate of dissolution in water. Therefore, it is important that this property of the glass be measured and related to the factors which effect it, such as composition, conditions of preparation, and conditions of exposure to water.

For several years, leaching tests have been conducted on small specimens of glass (less than 10 grams) containing radioactive nuclides. Most of these tests were done by immersing the glass in distilled water in polythene envelopes. Each day the specimens were transferred to fresh water in new envelopes. The amount of activity released from the glass was measured by counting a sample of the water, and the leaching rate was expressed as grams of glass/cm.²-day. Although it was known that all the components of the glass did not leach at the same rate, this method of expressing an apparent leaching rate was simple and adequate for comparing glasses of different compositions. The lowest leaching rate measured by these tests was 5×10^{-9} gm./cm.²-day, for a nepheline syenite-15% lime glass containing Ru-106 as the tracer nuclide. For glasses of other compositions the rates were as high as 1×10^{-5} gm./cm.²-day.

The major difficulties in doing leaching tests were found to be sampling and analysis. Since the rate of attack on glass was very low, the concentration of leached material in the water was as low as 0.005 ppm. As a result of this low concentration, inconsistencies were found in testing the small samples and it was thought necessary to improve the method.

The tests now being done in flowing water systems are improved in the following ways:

1. The glass has a higher specific activity.
2. The ratio of surface area of glass to water volume is higher.
3. The glass specimens are much larger and have surface areas up to 500 times those of the smaller specimens. This reduces the possibility of minor disturbances affecting the tests to an appreciable extent. To obtain large surface areas other workers have used powdered glass for leaching tests. Two of the major difficulties for this technique which make it undesirable are (a) determining the surface area, and (b) separating the entrained solids from the leaching solutions.

Figure 7 is a plot of leaching rate against time for two separate tests on groups of four 2-kg. blocks. This shows an initially rather high rate which decreased in three weeks by a factor of 500 to 1×10^{-7} gm./cm.²-day. These rates are typical of nepheline syenite glass containing 15% lime and 1.5% solids from the fission product solution. The amount of fission products released from glass leaching at these rates is so small that direct burial in the ground might be acceptable.

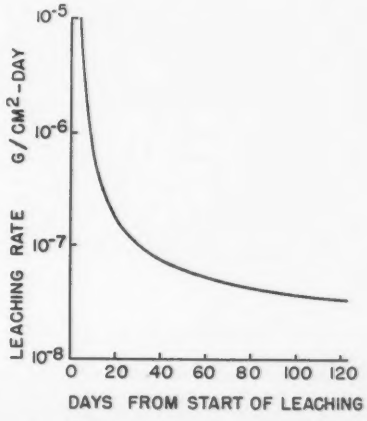

Figure 7 — Leaching rate of glass. Nepheline syenite — 15% lime.

Currently glasses of different compositions are being leached. Tests are also being made in the laboratory to measure the retention of leached nuclides on sand. Twenty-five 2-kg. pieces of glass containing about 300 curies of fission products have been buried in the field. Samples of the ground water nearby are taken periodically, but not enough data are yet available to estimate the rate of release of fission products from this glass.

CONCLUSION

Glass, a stable solid, is a desirable medium for the disposal of fission products. If the glass is exposed to water while it is buried in the ground it should release fission products only at an extremely low rate. The process being studied at Chalk River for the incorporation of fission products into glass appears to be suited to large scale operation. Development studies will be continued.

References

The following reports, issued by Atomic Energy of Canada Limited, Chalk River, Ont., are related to the disposal of fission products in glass:

White, J. M., and Lahaie, G. "Ultimate Fission Product Disposal. The Disposal of Curie Quantities of Fission Products in Siliceous Materials", Publication AECL–391 (1955).

Durham, R. W. "Disposal of Fission Products in Glass", Paper presented at the Second Nuclear Engineering and Science Conference, Philadelphia, Pa., March 11-14, 1957. Publication AECL–476.

Erlebach, W. E., and Durham, R. W. "The Behavior of Ruthenium in the Fixation of Fission Products", Paper presented at the Fourth Nuclear Engineering and Science Conference, Chicago, Ill., March 17-21, 1958. Publication AECL–681.

Watson, L. C., Rae, H. K., Durham, R. W., Evans, E. J., and Charlesworth, D. H. "Methods of Storage of Solids Containing Fission Products", Publication AECL–649 (1958).

Watson, L. C., Durham, R. W., Erlebach, W. E., and Rae, R. K. "The Disposal of Fission Products in Glass", Paper No. 195 presented to the Second International Conference of the Peaceful Uses of Atomic Energy, Geneva, Switzerland, Sept. 1-12, 1958, Publication AECL–605.

Bancroft, A. R., and Gamble, J. D. "Initiation of a Field Burial Test of the Disposal of Fission Products Incorporated into Glass", Publication AECL–718 (1958).

Watson, L. C., Bancroft, A. R., Gamble, J. D., Leaist, G. T., and Nishimura, D. T. "Equipment and Method of Operation for Incorporation of Fission Products into Glass", Publication AECL–756 (1958).

Durham, R. W., and Bell, D. "The Durability of Some Silicate Glasses That Could be Used in Fission Product Disposal", Publication AECL–817 (1958).

★ ★ ★

A Simplified Method for Determination of Solid Diffusion Coefficient with Non-Linear Adsorption Isotherm[1]

CHI TIEN[2]

A simplified method is proposed which enables the determination of solid diffusion coefficient for systems with non-linear adsorption isotherm. The method involves the approximation of the concentration history of the liquid phase with polynominal functions and consequently the match of the experimental results and calculated values. Experimental work has given rather satisfactory results.

In the study of rate processes of heterogeneous systems involving solid and fluid, like adsorption or ion exchange operations, the knowledge of the diffusion coefficient of the solute into the solid phase is of primary importance. This is especially true if the solid diffusion is the dominant factor in the overall mass transfer mechanism.

One of the several common methods which are used for measuring the diffusion coefficient of solid is by the sorption from a constant and limited volume of well-stirred fluid. By this method the progress of sorption can be easily followed. On the other hand, solution of the diffusion equation for the appropriate boundary conditions, leads to a theoretical expression for the progress of sorption in terms of parameter D.t. Comparisons of the theoretical curve and actual curve would yield the numerical value of D, the diffusion coefficient. The detailed description of this method has been reported in several publications [1, 2, 3].

One restriction imposed on this method is the distribution coefficient of the solute in the fluid and solid phases has to be constant or, in other words, the adsorption or equilibrium relationship should be linear. This is necessitated by the fact that only in the case of constant distribution coefficient can the solution of the corresponding diffusion equation be obtained. Unfortunately a larger number of systems exhibit non-linear behavior. It has been suggested [1] that in case of non-linear systems a differential technique could be used. However, this method, just like any other differential method, requires precision set-up and often gives unreliable results.

The object of this investigation is to present a method which enables the determination of solid diffusion coefficient for non-linear system by the utilization of the information of sorption from a finite and constant volume of well-stirred fluid. This is accomplished by substituting a dependent variable as an independent boundary condition. The detailed description is given in the next section.

[1]*Manuscript received May 19; accepted August 29, 1959.*
[2]*Department of Chemical Engineering, Essex College, Assumption University, Windsor, Ont.*
Contribution from the University of Tulsa, Tulsa, Oklahoma.

Mathematical Development

The diffusion of solute from a finite and constant volume of well-stirred fluid into initially empty spherical particles can be described as follows:

$$\frac{\partial q}{\partial t} = D\left[\frac{\partial^2 q}{\partial r^2} + \frac{2}{r}\frac{\partial q}{\partial r}\right] \quad \ldots\ldots(1)$$

$$C = C_o \quad q = O \quad O < r < a \text{ for } t < O \quad \ldots\ldots(2)$$

$$q = \alpha C \text{ at } r = a \; t > O \quad \ldots\ldots(3)$$

$$V_l\frac{\partial C}{\partial t} = K D\frac{\partial q}{\partial r} \; r = a \; t > O \quad \ldots\ldots(4)$$

The assumptions involved are: (a) the spherical particle is assumed to be quasi-homogeneous in structure, (b) the diffusion constant, D, is assumed to be constant, and (c) the desorption process is insignificant. The word, well-stirred, means that the concentration in the fluid phase is uniform at any time and, furthermore, because of the rigorous agitation, the resistance to the diffusion process due to the liquid film is negligible. This also implies that the solute at the surface of the particle is in equilibrium with that in the fluid phase.

Solutions of Equation (1) with boundary conditions given by Equations (2), (3) and (4) have been given by Carslaw and Jaeger[4], by Wagner [5], and by Wilson [6] for the case of constant distribution coefficient. For the case where α is a function of concentration, the resulting integral equation becomes non-linear and the solution becomes not obtainable.

As can be seen from Equations (1), (2), (3) and (4), a complete solution would give the expression of q, the solid phase concentration, as a function of time and position (inside the spherical particle) and an expression of C, the fluid phase concentration, as a function of time. The relationship between q and C is given by Equation (4) and, furthermore, neither of them is independent.

This problem, however, can be greatly simplified if the fluid concentration is known. In that case, with the assumption of equilibrium between the fluid phase and the surface of solid particle, q_s can be obtained in conjunction with the particular absorption isotherm. Furthermore q_s can be approximated as a function with polynominal expression of degree m or

$$q_s = q_s(t) = \sum_{i=0}^{m} P_i t^i \quad \ldots\ldots(5)$$

It should be noted the coefficients, P_i's can only be determined from direct experimental observation.

With q_s given by Equation (5), solution of the original diffusion equation is found to be:

$$q = -\frac{2D}{ra}\sum_{n=1}^{\infty}(-1)^n n\pi e^{-D\frac{n^2\pi^2}{a^2}t}\,\mathrm{Sin}\frac{n\pi r}{a}\int_0^t e^{D\frac{n^2\pi^2}{a^2}\lambda}\,q_s(\lambda)\,d\lambda = \sum_{i=0}^{m} P_i t^i - \left(\sum_{i=1}^{m} i\,P_i\,t^{i-1}\right)\left(\frac{2a^3}{D\pi^3 r}\right)\sum_{n=1}^{\infty}\frac{(-1)^{n+1}}{n^2}\,\mathrm{Sin}\left(\frac{n\pi r}{a}\right) +$$

$$\left(\sum_{i=2}^{m} i(i-1)\,P_i\,t^{i-2}\right)\left(\frac{2a^5}{D^2\pi^5 r}\right)\sum_{n=1}^{\infty}\frac{(-1)^{n+1}}{n^5}\,\mathrm{Sin}\left(\frac{n\pi r}{a}\right) + \ldots\ldots\ldots + (-1)^m(m!)\,P_m\,\frac{2a^{2m+1}}{D^m\pi^{2m+1}r}\sum_{n=1}^{\infty}\frac{(-1)^{n+1}}{n^{2n+1}}\,\mathrm{Sin}\left(\frac{n\pi r}{a}\right) +$$

$$\sum_{n=1}^{\infty}(-1)^n\,\mathrm{Sin}\frac{n\pi r}{a}\cdot e^{-D\frac{n^2\pi^2}{a^2}t}\left[P_o\frac{2a}{n\pi r} - P_i\left(\frac{2a}{n\pi r}\right)\left(\frac{a^2}{Dn^2\pi^2}\right) + 2P_2\left(\frac{2a}{n\pi r}\right)\left(\frac{a^2}{Dn^2\pi^2}\right)^2 + \ldots\ldots(-1)^m\,m!\,P_m\left(\frac{2a}{n\pi r}\right)\left(\frac{a^2}{Dn^2\pi^2}\right)^m\right] \quad \ldots\ldots(6)$$

Use the following relationships for $0 < x < \pi$,

$$\sum_{n=1}^{\infty}\frac{(-1)^{n+1}}{n}\,\mathrm{Sin}\,nx = -\frac{x}{2} \quad \ldots\ldots(7a)$$

$$\sum_{n=1}^{\infty}\frac{(-1)^{n+1}}{n^3}\,\mathrm{Sin}\,nx = -\left(\frac{1}{2}\right)\frac{x^3}{3!} + \left[\sum_{n=1}^{\infty}\frac{(-1)^{n+1}}{n^2}\right].x \quad \ldots\ldots(7b)$$

and

$$\sum_{n=1}^{\infty}\frac{(-1)^{n+1}}{n^{2m+1}}\,\mathrm{Sin}\,nx = \sum_{i=0}^{m}(-1)^{m+1}\frac{A_{2i}\,x^{2(m-i)+1}}{[2(m-i)+1]!} \quad \ldots\ldots(7)$$

where

$$A_{2i} = \sum_{n=1}^{\infty}\frac{(-1)^{n+1}}{n^{2i}} \qquad i > 0 \quad \ldots\ldots(8)$$

$$A_o = \left(\frac{1}{2}\right)$$

This gives

$$q = \sum_{i=0}^{m} P_i\,t^i - \left[\sum_{i=1}^{m} P_i\,t^{i-1}\right]\left(\frac{2}{D}\right)\left[-\frac{1}{2.3!}r^2 + A_2\frac{a^2}{\pi^2}\right] - \left[\sum_{i=2}^{m}(i)(i-1)\,P_i\,t^{i-2}\right]\left(\frac{2}{D^2}\right)\left[\left(\frac{1}{2}\right)\frac{r^4}{5!} - A_2\frac{r^2a^2}{(3!)\,\pi^2} + A_4\frac{a^4}{\pi^4}\right] +$$

$$\ldots\ldots\ldots + (-1)^m(m!)\,P_m\left(\frac{2}{D^m}\right)\sum_{i=0}^{m}(-1)^{m+i}\frac{A_{2i}\,r^{2m}\left(\frac{a}{r\pi}\right)^{2i}}{[2(m-i)+1]!} + \sum_{n=1}^{\infty}(-1)^n\,\mathrm{Sin}\left(\frac{n\pi r}{a}\right)e^{-D\frac{n^2\pi^2}{a^2}t}\left[P_o\frac{2a}{n\pi r} - P_i\frac{2a}{n\pi r}\left(\frac{a^2}{Dn^2\pi^2}\right) + \right.$$

$$\left. \ldots\ldots + (-1)^m\,m!\,P_m\left(\frac{2a}{n\pi r}\right)\left(\frac{a^2}{Dn^2\pi^2}\right)^m\right] \quad \ldots\ldots(9)$$

Let $q_{av.}$ be the amount of solute adsorped per unit mass of solid, $q_{av.}$ is given by the following expression:

$$q_{av.} = \frac{4\pi}{\frac{4}{3}\pi a^3}\int_0^a q(r\,t)\,r^2\,dr \quad \ldots\ldots(10)$$

Substitute Equations (9) into (10) and after rearrangement we have

$$\frac{q_{av.}}{q_s} = 1 - 6\,\Phi_1(t)\left(\frac{a^2}{D.t}\right)\left[-\left(\frac{1}{2}\right)\frac{1}{3!}\frac{1}{5} + A_2\frac{1}{3\pi^2}\right] + 6\,\Phi_2(t)\left(\frac{a^2}{D.t}\right)\left[\left(\frac{1}{2}\right)\frac{1}{5!}\frac{1}{7} - A_2\left(\frac{1}{3!}\right)\left(\frac{1}{5\pi^2}\right) + A_4\frac{1}{3\pi^4}\right] + \ldots\ldots +$$

$$(-1)^m\,\Phi_m(t)\left(\frac{a^2}{D.t}\right)^m\sum_{i=0}^{m}\frac{(-1)^{m+i}\,A_{2i}}{[2(m-i)+3](2\pi)^{2i}[2(m-i)+1]!} -$$

$$6\,\frac{\sum_{n=1}^{\infty}\left[P_o - P_1 t\left(\frac{a^2}{D.t}\right)\frac{1}{n^2\pi^2} + \ldots\ldots(-1)^m m!\,P_m\,t^m\left(\frac{a^2}{D.t}\right)^m\left(\frac{1}{n^2\pi^2}\right)^m\right]\cdot\frac{e^{-D\frac{n^2\pi^2}{a^2}t}}{n^2\pi^2}}{\sum_{i=0}^{m}P_i\,t^i} \quad \ldots\ldots(11)$$

where

$$\Phi_1(t) = \frac{\sum_{i=1}^{m} i\, P_i\, t^i}{\sum_{i=0}^{m} P_i\, t^i} \quad \ldots\ldots\ldots\ldots\ldots\ldots (12)$$

$$\Phi_2(t) = \frac{\sum_{i=2}^{m} i(i-1)\, P_i\, t^i}{\sum_{i=0}^{m} P_i\, t^i} \quad \ldots\ldots\ldots\ldots\ldots\ldots (13)$$

$$\Phi_m(t) = \frac{m!\, P_m\, t^m}{\sum_{i=0}^{m} P_i\, t^i} \quad \ldots\ldots\ldots\ldots\ldots\ldots (14)$$

With the surface concentration known, $q_{av.}/q_s$ can be plotted against time with $a^2/D.t$ as parameter. This would result in a series of curves. On the other hand, from the experimental results, $q_{av.}/q_s$ can be plotted against time. This experimentally obtained curve will intersect the computed curves at a number of points. Each of these points is specified by particular values of t and $a^2/D.t$. This in turn gives the numerical value of D. Furthermore, a consistant value of D would prove the validity of the assumption that the diffusion coefficient is constant. An illustrative example will be given in the next section to demonstrate the detailed procedure.

Illustrative Example

The adsorption of oxalic acid from glycol solution with Permutit SKB has been studied [5]. For a particular run, the following results were obtained:

To 500 cc. of glycol solution with $C_o = 0.0512$ millequivalents of oxalic acid per cu. cm., 2.7 grams (dry basis) of Permutit SKB were added and vigorously agitated to eliminate the resistance of the liquid film. The resin when completely wet was 0.049 inches in diameter. The concentration of the liquid at various times was determined from periodic titration.

Time Sec.	C/C_o	q_s	q_{av}/q_s
300	0.811	4.89	0.368
600	0.740	4.76	0.517
1000	0.665	4.64	0.700
1800	0.579	4.46	0.906
3000	0.536	4.36	1.000
4500	0.524	4.34	—

Values of q_s were obtained with the information of adsorption isotherm of the system. q/q_s were found by material balance.

The surface concentration q_s, as a function of time, is approximated by a simple polynominal of second degree. The equation is found to be:

$$q_s = 4.832 - 2.06 \times 10^{-4} t + 2.12 \times 10^{-8} t^2 \quad \ldots\ldots (15)$$

The comparison between the actual value of q_s and that given by this approximation is presented in Table 1. Generally speaking, values of q_s as given by Equation (15) are lower than the actual value for the lower value of time and are higher for higher values of time.

TABLE I

Comparison between actual surface concentrations and values given by approximation.

Time (Rec.)	Surface Concentration, q_s	
	Actual	Approximate
300	4.62	4.535
600	4.55	4.5
1000	4.47	4.455
1800	4.33	4.335
3000	4.26	4.31
4500	4.24	4.27

With q_s given by Equation (15), Equation (11) reduces to:

$$\frac{q_{av}}{q_s} = 1 - 6\Phi_1(t)\left(\frac{a^2}{D.t}\right)\left(\frac{1}{15}\right) + 6\Phi_2(t)\left(\frac{a^2}{D.t}\right)^2\left(\frac{2}{945}\right) - \left[\frac{P_o}{\sum_{i=0}^{2} P_i t^i} \cdot \sum_{n=1}^{\infty} \frac{e^{-D\frac{n^2\pi^2}{a^2}t}}{n^2\pi^2} + \frac{P_i t}{\sum_{i=0}^{2} P_i\, t^i}\left(\frac{a^2}{D.t}\right)\sum_{n=1}^{\infty}\frac{e^{-D\frac{n^2\pi^2}{a^2}t}}{n^4\pi^4} + \frac{2P_2 t_2}{\sum_{i=0}^{2} P_i\, t^i}\left(\frac{a^2}{D.t}\right)^2 \sum_{n=1}^{\infty}\frac{e^{-D\frac{n^2\pi^2}{a^2}t}}{n^6\pi^6}\right] \quad \ldots\ldots (16)$$

$$\Phi_1(t) = \frac{t[-2.06 \times 10^{-4} + 4.24 \times 10^{-8}\, t]}{4.832 - 2.06 \times 10^{-4} t + 2.12 \times 10^{-8} t^2}$$

$$\Phi_2(t) = \frac{4.24 \times 10^{-8} t^2}{4.832 - 2.06 \times 10^{-4} t + 2.n \times 10^{-8} t^2} \quad \ldots\ldots (17)$$

Numerical values of q/q_s corresponding different time and preassigned value of $D.t/a^2$ were computed from Equation (17) and graphically presented in Figure 1. On the same chart, the curve relating q/q_s and time and observed from the experimental work was superimposed. This latter curve intersects the calculated values of q/q_s at the following points:

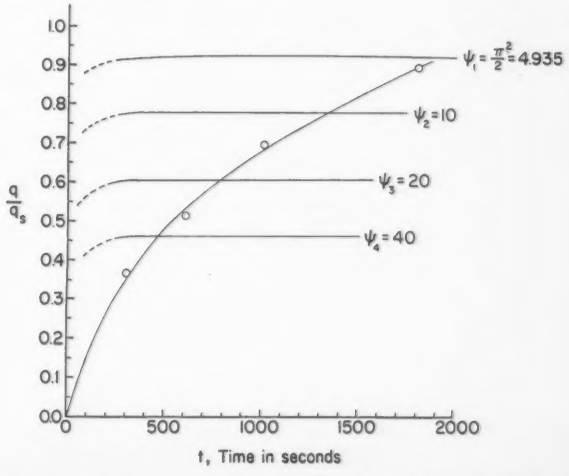

Figure 1—Analysis of experimental data for determination of diffusional coefficient.

Time – Sec.	$a^2/D.t$	D
482	40	$5.25 \times 10^{-5}a^2$
802	20	$5.24 \times 10^{-5}a^2$
1340	10	$6.67 \times 10^{-5}a^2$
		$5.83 \times 10^{-5}a^2$

$a = 0.0245$ in.
$D = 2.256 \times 10^{-7}$ cm²/sec.

In this particular case, D was found to be increasing with time, however, in other cases, the opposite trend was observed. Since no definite trend exists, a simple arithmetic average was taken. It is felt that at least part of the deviation is due to the inaccurate approximation of q_s.

Conclusions

A simplified method is proposed which enables the determination of the solid diffusion coefficient for systems with non-linear adsorption isotherm. This method requires very simple experimental set-up and the results from limited work seem to be rather satisfactory.

Nomenclature

- a = Radius of spherical particle
- C = Concentration in fluid phase
- C_o = Initial concentration in the fluid phase
- D = Diffusion coefficient
- K = Product of the total surface area of solid particle and its density
- P_i = Coefficients of the i-th term in the polynomial expression for surface concentration
- q = Concentration in solid phase, based on per unit mass of solid
- q_{av}, = Amount of solute adsorped, per unit mass of solid
- q_s = Surface concentration, based on the per unit mass
- r_s = Radial distance from the centre of the spherical particle
- t = Time
- V = Volume of total fluid
- α = Distribution coefficient

References

(1) Carman, P. C., and Haul, R. A., Proc. Roy. Soc., **222,** 109, 1954.
(2) Crank, J., Phil. Mag., **39,** 140, 1948.
(3) Grober, H., Zeit. Verienes Deutch Ing., **69,** 705, 1925.
(4) Carslaw, H. S., and Jaeger, J. C., Conduction of Heat in Solids, Oxford University Press (1948).
(5) Wagner, C., 1945, See Zimens, K. E., Ark. Kemi. Min. Geol.
(6) Wilson, A. H., Phil. Mag., **39,** 48, 1948.
(7) Tien, C., Ph.D. Thesis, Northwestern University (1958).

★ ★ ★

Nuclear Grade Uranium Tetrafluoride by the Moving Bed Process[1]

F. H. HUESTON[2]

After two years of research and development in the pilot plant stages, a plant for the production of nuclear grade uranium tetrafluoride by the Moving Bed Process has been designed, built, and successfully operated at Eldorado's Port Hope Refinery. This is the only production facility in the world using the moving bed technique for the production of UF_4.

An exceptionally high grade uranium tetrafluoride, low in unconverted uranium oxides and uranyl fluoride can be obtained. A large percentage of the production exceeds 99% uranium tetrafluoride. Total metal contamination is less than 150 ppm.

URANIUM tetrafluoride is produced by a three-step process from uranium trioxide; UO_3 is produced at Port Hope by the Solvent Extraction Process (1). (See Figure 1).

The first step in the hydration of the UO_3 and the casting of the resultant slurry into pellets; next comes the reduction of the hydrate to UO_2 in a moving bed reactor by a countercurrent flow of hydrogen; and finally there is the hydrofluorination of UO_2 with a countercurrent flow of gaseous hydrofluoric acid.

[1]*Manuscript received June 9; accepted October 22, 1959.*
[2]*Development Engineer, Eldorado Mining and Refining Limited, Port Hope, Ont.*

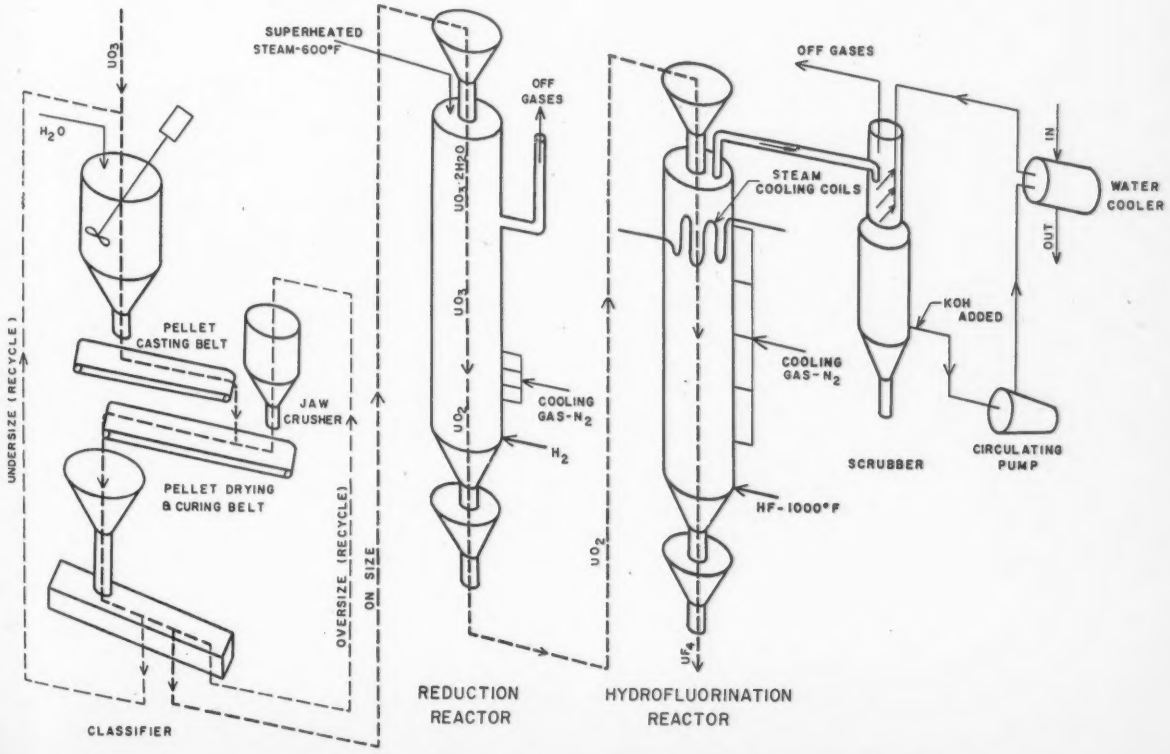

Figure 1—Production of uranium tetrafluoride moving bed process flow sheet.

Previous Work

Original laboratory studies on the feasibility of this process are described by J. E. Moore [2].

Laboratory bench scale studies were carried out by Le Gassie [3] et al at U.S.A.E.C. laboratories at New Brunswick, New Jersey.

A great deal of work on the evaluation of the moving bed process was performed at the U.S.A.E.C. plant run by National Lead Company, Fernald, Ohio. A summary of this work was given by Arnold et al [4] at the recent Geneva 'Atoms for Peace' Conference. The project at Fernald was shelved in 1957.

A pilot plant with two 8-in. diameter reactors was constructed at the Port Hope Refinery in the fall of 1956 and operations started in December of the same year. Melvanin [5] discussed the layout and operating conditions of the plant.

It took about 18 months to overcome the production problems; and in the Spring of 1958 it was decided to construct a production scale plant. A very tight schedule was laid out, and Catalytic Construction Company, the constructor of the pilot plant, was retained to design and build the new plant in conjunction with Eldorado personnel. The new plant started on December 11, 1958 and produced specification product before the end of the year.

Theoretical Discussion

It is not the intention here to discuss the general theory behind moving bed reactors, as this has been adequately covered elsewhere [7].

The first step in the process is the formation of hydrate pellets according to the following reaction*:

$$UO_3 + 2H_2O \rightarrow UO_3.2H_2O + \text{Heat} \quad \ldots\ldots(1)$$

The reason for making the pellets is two-fold. Firstly, a feed in a discrete form must be fed to the reactors to avoid packing. Secondly, research investigations have shown that the hydrate is a more reactive feed material than the UO_3. One theory is that the hydrate pellet has its moisture removed in the first stage of treatment and is left quite porous, therefore offering a large surface area for gaseous contact in subsequent reaction:

$$UO_3 2H_2O + \text{Heat} \rightarrow UO_3 + 2H_2O \quad \ldots\ldots(2)$$

The third step may be accomplished in one of two ways. The first is a direct hydrogen reduction:

$$UO_3 + H_2 \rightarrow UO_2 + H_2O + \text{Heat} \quad \ldots\ldots(3)$$

The second is a two stage process—a thermal reduction followed by the hydrogen reduction:

$$6\ UO_3 + \text{Heat} \rightarrow 2\ U_3O_8 + O_2 \quad \ldots\ldots(4)$$

$$U_3O_8 + 2H_2 \rightarrow 3UO_2 + 2H_2O + \text{Heat} \quad \ldots\ldots(5)$$

There is very little control over which way the reduction takes place. Gas consumption data indicates it is finally accomplished partly as shown in both reactions. Some typical figures are given in Table 1.

The fourth step is hydrofluorination. The main and desirable reaction in the hydrofluorination reactor is:

$$UO_2 + 4HF \rightarrow UF_4 + 2H_2O + \text{Heat} \quad \ldots\ldots(6)$$

An undesirable side reaction, caused by unconverted UO_3 or U_3O_8 forming uranyl fluoride also takes place:

$$UO_3 + 2HF \rightarrow UO_2F_2 + H_2O + \text{Heat} \quad \ldots\ldots(7)$$

$$U_3O_8 + 8HF \rightarrow UF_4 + 2UO_2F_2 + 4H_2O + \text{Heat} \quad \ldots\ldots(8)$$

*The hydrates of uranium trioxide are discussed by Bright and Jongejan (8). It is questionable whether the dihydrate is the only hydrate present.

TABLE 1

GAS CONSUMPTION DATA FOR THE CONVERSION OF UO_3 TO UO_2 IN A MOVING BED REACTOR

Product Rate lbs. Per. Hr.	Flow of Dissociated Ammonia in Cu. Ft. per. H.*	Percent of theoretical basis UO_3 — UO_2 Reduction
125	200	90.8
175	285	92.2
220	360	93.0
270	470	98.2

*Reduced to N.T.P.

Because of these side reactions, extreme care must be taken to complete the reduction phase, and to protect adequately the hydrofluorination reaction from the air. This is done by blanketing the reactor with inert gas.

Eldorado Development

One of the greatest problems in the pilot phase was the development of equipment which would make pellets of sufficient reactive qualities to produce a high grade UF_4 from the gas-solids reactions to follow.

Previous work in the U.S. by Henline [6] indicated that cast pellets appeared to be highest in reactivity with regard to the conversion to UF_4. Preliminary work at Port Hope indicated that this was so, in as much as the commercial pellet machines that were tried produced unsatisfactory pellets. In every case, the unequal hardness of pellets due to concentric layering and/or too high a density caused poor conversion from UO_2 to UF_4 by inhibiting the diffusion of the anhydrous hydrofluoric acid throughout the pellets. Eventually, it became necessary to abandon the commercially available machines and develop separate techniques and equipment.

The preliminary design of the reduction reactor proved to be quite good and only minor changes were required to make this process trouble-free.

The major problem in the hydrofluorination reactor was the maintenance of a continuous flow through the equipment. During the reaction from UO_2 to UF_4 a 30% expansion takes place and tends to cause bridging if the reaction rate becomes too rapid at any one time, in any portion of the reactor. There is also a tendency for the pellets to soften during the conversion period. The placing of vibrators at key locations on the reactor walls and the development of proper operating techniques greatly reduced the plugging tendencies in the reactor.

DESCRIPTION OF EQUIPMENT AND PROCESS

Pelleting Equipment

Uranium trioxide powder is continuously fed by an adjustable screw feeder into a mixing vessel into which a controlled volume of water is also fed. The resultant slurry flows continuously onto a rubber casting belt, which is approximately 21 ft. long and runs at 10 ft. per minute through a controlled climate cabinet maintained at a temperature of 180°F. and a relative humidity of +90%. At the end of this belt the pellets are knocked out of their cavities by a rotating mechanical device. They discharge onto a curing belt moving at approximately 2/3 ft. per minute in a direction opposite to the casting belt. In this operation, a temperature of 70-80°F. is maintained, and a relative humidity set to facilitate removal of excess moisture from the pellets. (See Figure 2).

Figure 2 — Pellet casting and curing equipment. Note: Screw feeder for oxide additions and flowrator for the water. Part of dust collection duct work may be seen at the far end.

The whole pelleting operation is enclosed in a dust-tight cabinet with dust collection facilities to prevent contamination of the plant air with uranium dust.

The pellets are of a pyramidal diamond shape, approximately 5/8 in. long, 3/8 in. wide and 3/16 in. deep at the base. The unit has a capacity of 1000 lb. of hydrated pellets per hour. This is sufficient to maintain 24-hour, seven-day design capacity operation of the reactors by operating a 16-hour, five-day week.

Reduction Reactor

The reduction reactor is a 14-in. internal diameter vessel, approximately 16 ft. high. It has a gas disengaging section located 4 ft. from the top of the reactor for the release of off-gases from the resulting reactions. (See Figure 3). Design capacity is one mole per hour of UO_2 (270 lb.). Superheated steam at 600°F. and 7 in. W.C. pressure is admitted concurrently at the top of the reactor along with the pellets. This dehydrates the pellets for the gas-solids reaction to follow. Because of the presence of small quantities of nitric acid, the top 4 ft. of the reactor is type 347 stainless steel. The remainder of the reactor is 309.

The actual reduction from UO_3 *to* UO_2 is carried out in the lower portion of the reactor at 1000-1100°F. The reducing media is dissociated or "cracked" ammonia ($3H_2 + 1N_2$) which is generated by passing anhydrous ammonia over a nickel catalyst at 1700°F. Temperature of the reaction is controlled by the introduction of a blanketing gas which analyzes +90% nitrogen, 8% carbon dioxide and small quantities of hydrogen and carbon monoxide. This gas is produced by the controlled combustion of natural gas with air in a furnace, with the product gases being collected and compressed to 150 p.s.i.g. for use.

The reactor is heated electrically by three jackets, each with a maximum output of 20 kw. The power to the jackets is set to maintain stipulated bed temperatures throughout the reactor. A unique switching arrangement allows the choice of six levels of heat to maintain conditions and prevent heavy on-off demand for power and consequent cyclic thermal conditions in the reactor wall. Table 2 gives some typical data with regard to operation of the reactor.

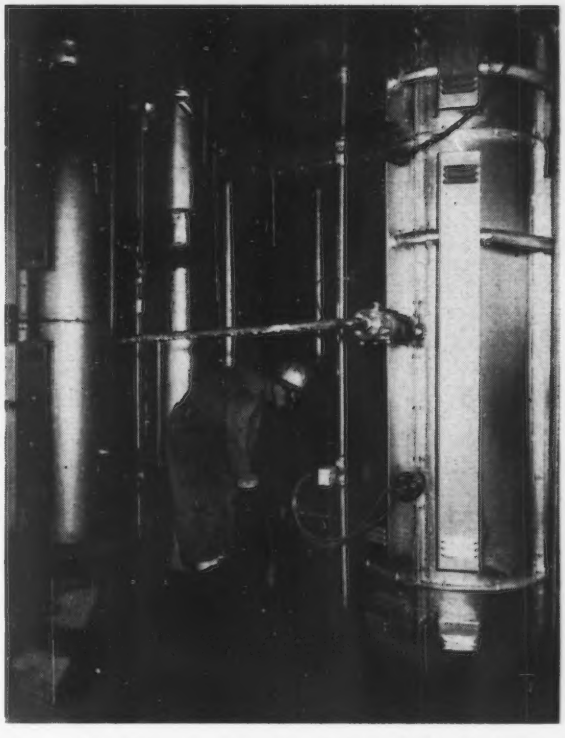

Figure 3 — General view of reactors. Hydrofluorination reactor on the right and reduction on the left.

TABLE 2

OPERATING FLOWS AND PRESSURES IN THE REDUCTION REACTOR AT VARIOUS THROUGHPUTS

Product rate lb. per hr.	Solids rate ft. per hr.	Gas velocity ft. per sec.* (void space)	$\triangle P$ in in. *W.C.* bottom of reactor to disengaging section
125	0.70	0.50	7
175	0.98	0.82	9
220	1.3	1.48	12
270	1.5	2.70	18

*Large temperature differences inside the reactor make calculation of actual velocities virtually impossible. For comparison purposes velocities are calculated assuming atmospheric pressure and 700°F. This figure includes both the dissociated ammonia for reduction and the sealing and cooling gases. The bed porosity averages 0.28.

The Hydrofluorination Reactor

The hydrofluorination reactor is 24 ft. high and 14-in. internal diameter. Its design capacity is one mole of UF_4 per hour (314 lb.). This reactor is made entirely of Inconel and is equipped with three sets of cooling coils using low-pressure steam as the cooling medium. The steam discharged from these coils is super-heated from the pick-up and is used in the reduction reactor for dhydration. The reactor is also equipped with five blanket-gas spargers to control hot spots in the reactor. (See Figure 3). Hydrofluoric acid vapor at 1100°F., is fed into the bottom of the reactor and flows countercurrently to the pellets. The acid is heated first in a steam jacketed carbon steel tank, which vaporizes the acid and heats it to 140°F. A six-pass Monel Brown Fintube raises the temperature of the acid to 275°F. and a 35 kw electric furnace with an Inconel coil heats the acid to 1100°F. The

reactor is equipped with five strategically placed vibrators to maintain steady flow throughout the reactor. Five electric jackets with a maximum heat output of 20 kw each are used for heating the reactor; they are controlled similarly to those on the reduction reactor. The temperature of the bed in the main reaction zone is set up at 1000-1100°F. Both reactors are controlled from a central control panel. (See Figure 4).

The stoichiometric excess acid from the reactor which runs about 10% passes through an off-gas line along with the excess blanketing gas and is scrubbed with aqueous caustic potash. The level in the scrubber is automatically controlled. In order to recover any entrained uranium carried over in the off-gas line, the effluent is filtered before being sent to waste disposal. Alkalinity in the scrubber liquor is controlled by continuous additions of 45% KOH by a small positive displacement pump.

The rate of product flow through each reactor is controlled by a specially designed belt feeder located at the bottom of each reactor. The belt is choke fed through a seal leg. Table 3 gives some typical data with regard to the operation of the reactor.

TABLE 3

OPERATING FLOWS AND PRESSURES IN THE HYDROFLUORINATION REACTOR AT VARIOUS THROUGHPUTS

Product rate lb. per hr.	Solids rate ft. per hr.	Gas velocity ft. per sec.*	$\triangle P$ in in. *W.C.* bottom of the reactor to off-gas line
150	0.93	1.23	15
190	1.17	1.86	23
250	1.55	2.61	35
290	1.80	3.35	55

*Large temperature differences inside the reactor make calculation of actual velocities virtually impossible. For comparison purposes velocities are calculated assuming atmospheric pressure and 700°F. This figure includes both *HF* vapor and sealing and cooling gases. It should be noted that velocities will fall after conversion of UO_2 to UF_4 because four moles of *HF* result in two moles of water being produced. The bed porosity averages 0.37.

Conclusions

Table 4 illustrates the progress made in the development of acceptable nuclear grade green salt.

TABLE 4

PROGRESS OF PRODUCTION OF HIGH GRADE URANIUM TETRAFLUORIDE

Start of run	Length of run hours	% UF_4	% *AOI*(a)	% UO_2F_2
Mar. 25, 1957 (b)	30	66.55	28.95	4.50
May 9, 1957	38	80.84	14.21	4.95
Aug. 13, 1957	104	89.10	7.52	3.33
Nov. 11, 1957	552	93.20	5.91	0.89
May 21, 1958	624	97.34	1.81	0.85
Aug. 7, 1958	696	97.81	1.39	0.80
Jan. 2, 1959(c)	Continuous	98.54	0.59	0.87
Mar. 1, 1959	Continuous	98.75	0.50	0.75

(a) Ammonium oxalate insoluble.
(b) First run of pilot plant.
(c) Production plant product.

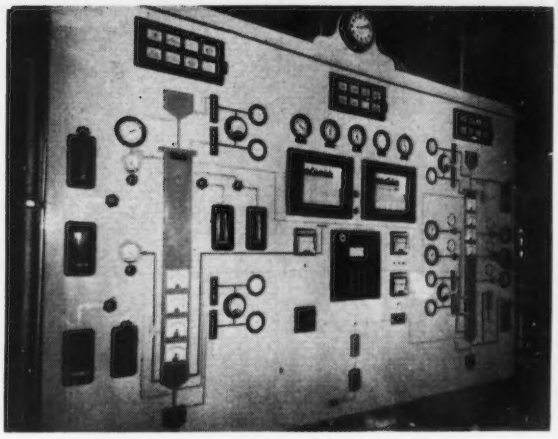

Figure 4—Reactor control panel. The left hand side controls the reduction reactor and the right the hydrofluorination reactor.

It may be noted that as development progressed the operation became much smoother, as indicated by the length of runs made.

From Table 4 it may be observed that the production of nuclear grade uranium tetrafluoride by the moving bed process is definitely feasible. It offers many economic advantages over some other methods presently adopted—especially in the use of reagent chemicals, and particularly in its adaptability for use in smaller sized production units.

Acknowledgment

The author acknowledges the assistance given to him by the Port Hope Staff, particularly Messrs. Berry, Currie and Walker.

References

(1) Burger, J. C., Jardine, J. McN., Atoms for Peace Paper P-228. (June 1958). Canadian Refining Practice in Production of Uranium Trioxide by Solvent Extraction with Tributyl Phosphate.

(2) Moore, J. E., USAEC Research and Development Report ORNL-54-12-169. (1954). Moving Bed Reactor Studies: A Literature Survey Concerning the One Step Production of UF_4.

(3) Le Gassie, R. W., Bertram, H. W., Roszkowski, E. S., Petretic, G. J., USAEC Research and Development Report NBL 105. (1955). Green Salt Moving Bed Process.

(4) Arnold, D. S., Henline, P. W., Sisson, R. H., Atoms for Peace Paper P-1015. (June 1958). A Moving Bed Reactor for the Production of Uranium Tetrafluoride.

(5) Melvanin, F. W., Atoms for Peace Paper P-229. (June 1958). Canadian Development Work with Moving Bed Reactors for the Reduction of Uranium Trioxide and Hydrofluorination to Uranium Tetrafluoride for Subsequent Production of Metal.

(6) Henline, P. W., Klee, A. J., Walter, E. J., USAEC Research and Development Report NLCO 651. (1956). Moving Bed Reactor Pellet Development Program.

(7) Vener, R. E., Chem. Eng. **62**, 175-206. (1955).

(8) Bright, N. F. H., Jongejan, A., Canadian Mines Branch Investigation Report IR-58-20. Examination of Certain Uranium Trioxide Hydrate Samples From Eldorado Mining and Refining Limited, Port Hope, Ontario, in Relation to their Pelleting Behavior.

★ ★ ★

Evaluation of Antoine Constants

BENJAMIN C.-Y. LU
Department of Chemical Engineering,
University of Ottawa, Ottawa, Ontario.

The Antoine equation

$$\log p = A - B/(C + t) \quad \ldots\ldots\ldots\ldots\ldots (1)$$

is found to be adequate for representing and extrapolating vapor pressure data. A method is proposed for evaluating the constants in which the approximate linear relationships of the Clausius-Clapeyron plot (log p vs. $1/T$) is employed. The proposed method provides a much less involved procedure than the available calculation methods [1, 2] and does not involve the selection of a base-point which is assumed to be free from error as required by the Thomson's graphical method [3].

The constant C may be obtained by evaluating the values of $d \log p/dt$ at any two temperatures. From Equation (1)

$$d \log p/dt = B(C + t)^2 \quad \ldots\ldots\ldots\ldots\ldots (2)$$

Therefore

$$(d \log p/dt)^{0.5}_{T_1}/(d \log p/dt)^{0.5}_{T_2} = (C + t_2)/(C + t_1) \ldots . (3)$$

and solve for C. However, it is not recommended to determine the values of the quantity $d \log p/dt$ on a log p vs. t plot, as slopes are difficult to determine accurately on such a plot. Instead, advantage is taken of the fact that on a Clausius-Clapeyron plot, the resulting curve shows much less curvature and it may be considered as linear over a small temperature range. In many instances, a complete curve over a moderate temperature range may be approximately represented by two straight lines. Two linear portions are taken from the plot and their slopes are used to evaluate the constant C.

$$\text{slope} = d \log p/d\,(1/T) = -(1/T^2)\,(d \log p/dT) = -(1/T^2)\,(d \log p/dt) \quad \ldots\ldots\ldots\ldots\ldots (4)$$

and

$$T_2\,[d \log p/d\,(1/T)]^{0.5}_{T_1}/T_1\,[d \log p/d\,(1/T)]^{0.5}_{T_2} = \frac{C + t_2}{C + t_1} . (5)$$

The quantity T is taken to be the temperature corresponding to the mid-point of the linear section.

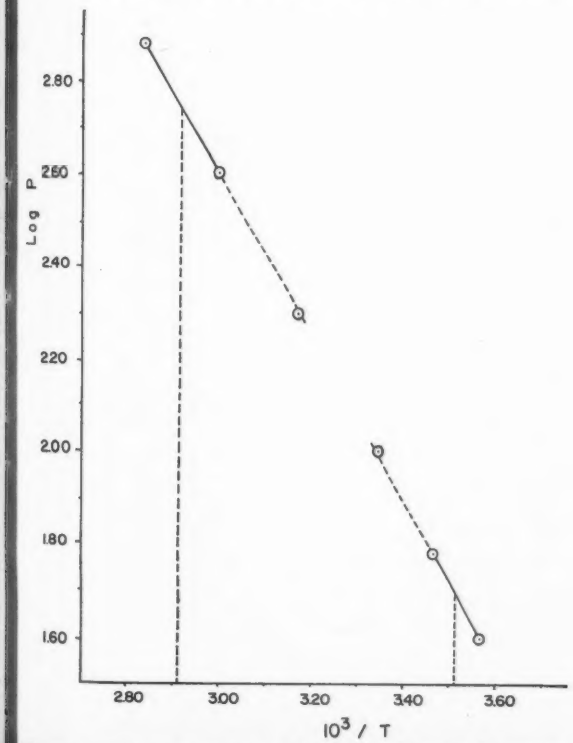

Figure 1—Vapor pressure of benzene (Clausius-Clapeyron plot).

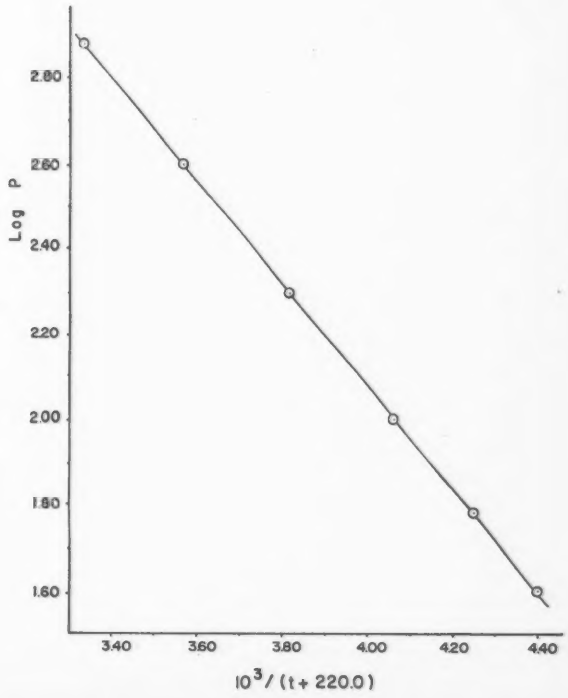

Figure 2—Vapor pressure of benzene (Antoine plot).

The vapor pressure data of benzene [4] are used to illustrate the procedure. Figure 1 illustrates the plot of log p vs. $1/T$, in which six points are employed. Two linear sections are taken on the plot corresponding to the first two points and the last two points as listed in Table 1.

$$\text{Slope I} = -1828.9, \quad 1/T_1 = 0.0035136, \quad t_1 = 11.45$$

$$\text{Slope II} = -1693.6, \quad 1/T_2 = 0.0029139, \quad t_2 = 70.03$$

Therefore

$$(C + 70.03)/(C + 11.45) = 1.2531$$

and

$$C = 220.0$$

This method of obtaining the constant C is believed to be simpler than the Thomson's graphical method in actual applications. It is especially useful when the vapor pressure data are only of moderate precision. The value of C is used to construct Fig. 2 where log p is plotted against $1/(C + 220.0)$, resulting a good straight line which can be conveniently extrapolated. The slope of this straight line is $(-B)$. The constant A may be evaluated by Equation (1). The constants A and B may also be solved by means of the equations

$$\Sigma \log p = n A - B \Sigma\, 1/(C + 220.0) \quad \ldots\ldots\ldots (6)$$

and

$$\Sigma \log p/(C + 220.0) = A \Sigma\, 1/(C + 220.0) - B \Sigma\, 1/(C + 220.0)^2 \quad \ldots\ldots\ldots\ldots\ldots (7)$$

where n is the number of experimental points employed in Figure 2. The values of A and B obtained are

$$A = 6.8948$$

$$B = 1204.6$$

The calculated vapor pressure data are compared in Table 1 with the values taken from the Perry's Handbook. It is evident that the agreement is very satisfactory.

TABLE 1

COMPARISON OF CALCULATED VAPOR PRESSURE WITH LITERATURE VALUES

t, °C.	p, mm. Hg. (4)	$\log p = 6.8948 - 1204.6/(220.0 + t)$	$p_{calc.}$	$p_{calc.} - p$
7.6	40	1.6024	40.0	0
15.4	60	1.7778	60.0	0
26.1	100	2.0002	100.0	0
42.2	200	2.3008	199.9	−0.1
60.6	400	2.6020	399.9	−0.1
80.1	760	2.8810	760.3	+0.3

Nomenclature

A, B, C = constants
p = vapor pressure, mm. Hg.
t = temperature, °C.
T = absolute temperature = $273.16 + t$

References

(1) Willingham, C. B., Taylor, W. J., Pignocco, J. M. and Rossini, F. D., J. Research Nat. Bur. Standards **35,** 219 (1945).

(2) Rose, A., Acciarri, J. A., Johnson, R. C. and Sanders, W. W., Ind. Chem. Eng. **49,** 104 (1957).

(3) Thomson, G. W., Chem. Review **38,** 1 (1946).

(4) Perry, J. H., "Chemical Engineers' Handbook", 3rd ed. p. 153, McGraw-Hill, New York, 1950.

★ ★ ★